Front. Struct. Civ. Eng. 2024, 18(12): 1865–1887
https://doi.org/10.1007/s11709-024-1127-6

RESEARCH ARTICLE

Rotary vibrating machine-based washing and sieving method for soil classification

Shengnan MA[a], Wendal Victor YUE[b], Zhongqi Quentin YUE[c*]

[a] *Department of Civil Engineering, The University of Hong Kong, Hong Kong 999077, China*
[b] *Department of Geotechnical Engineering, College of Civil Engineering, Tongji University, Shanghai 200092, China*
[c] *School of Science, Harbin Institute of Technology, Shenzhen 518055, China*
[*]*Corresponding author. E-mail: yueqzq@hku.hk*

ABSTRACT This study develops a machine-based washing and sieving method to accurately determine the soil particle size distribution for classification. This machine-based method is an extension of the recently developed and invented manual-based extended wet sieving method. It revises and upgrades a conventional rotary vibrating sieve machine with a steel sieve of aperture 0.063 mm and ten cloth sieves of apertures from 0.048 to 0.0008 mm for washing and sieving silt and clay. The machine generates three-dimensional motion and vibration, which allows particles smaller than the sieve aperture to pass through the sieve quickly. A common soil in Hong Kong, China, named completely decomposed tuff soil is used as test material for illustration. The silt and clay mixtures are successfully separated into many sub-groups of silt particles and clay particles from 0.063 to less than 0.0008 mm. The test results of the machine-based method are examined in detail and also compared with the manual-based method. The results demonstrate that the machine-based method can shorten the sieving duration and maintain high accuracy. The particle sizes of separated silt and clay particles are further examined with scanning electron microscopic images. The results further demonstrate that the machine-based method can accurately separate the particles of silt and clay with the pre-selected sieve sizes. This paper introduces a new machine-based washing and sieving method, and verifies the efficiency of the machine-based method, the accuracy of particle size, and its applicability to the classification of different types of soil.

KEYWORDS particle size, rotary vibrating sieve machine, cloth sieve, washing and sieving, silt, clay

1 Introduction

1.1 Conventional soil classification methods

Soil classification divides general soils into different categories mainly according to their particle size distribution (PSD) supplemented by plasticity and organic content for various purposes in engineering and science. Soil classification can disclose the soil behavior in a concise manner and guide engineering practices to find suitable soil for construction and deal with geological disasters correctly [1–3]. Some standardized soil classification systems such as BS 5930 [4], Geoguide 3 [5], and ASTM D2487-17 [6] have been developed for classifying soils into coarse soil or fine soil based on PSD also considering the soil plasticity (and/or organic or non-organic soil according to the organic content).

Article history: Received Jan 24, 2024; Accepted Apr 24, 2024

The wet sieving method is usually used for separating coarse particles larger than 0.063 mm (or 0.075 mm) from fine particles smaller than 0.063 mm (or 0.075 mm) [4–8]. For the further classification of coarse soil, the standard dry sieving method is used for separating the gravel and sand portion into several sub-size groups including coarse gravel, medium gravel, fine gravel, coarse sand, medium sand, and fine sand with a stack of steel sieves with apertures from 63 to 0.063 mm [7,8]. The particle size and particle properties of individual gravel and sand particles can be independently examined after dry sieving [9]. The plot of liquid limit and plasticity index remains the further criterion for classifying fine-grained soil [10].

1.2 Issues of conventional soil classification methods

The differences between coarse-grained soil and fine-grained soil classification methods can be caused by the limitations of classical sedimentation methods. The sedimentation methods assume the particle shape to be spherical and the flow to be laminar. This assumption and the physical principle-based calculation could underestimate the size of the silt and clay particles [11,12]. In addition, the existing two international cut-off sizes of silt and clay are 0.005 [7,13] or 0.002 mm [5,14], and are based on physical assumptions. The presence of two cut-off sizes could be attributed to the inability of the sedimentation method to obtain individual silt and clay particles from general soil for independent examinations.

For the sieving method, the particle size is defined as the length of an aperture through which a particle can just pass [8]. For sedimentation method, the particle size is defined as the diameter of an equivalent sphere settling with the same velocity and in the same liquid, and this method can underestimate the size of platy particles [8,12]. The inconsistency in the definition of particle size and physical assumptions can cause the PSD curve from a wet sieving test not to be joined up with that from a sedimentation test for the same material [15].

1.3 Motivation of this study

Ma et al. [16] used nylon filter cloths with apertures from 0.048 to 0.0008 mm to facilitate the division of silt and clay mixture into several sub-groups of silt and clay materials. This method can also enable the particle size definition of silt and clay particles using cloth sieve sieving method to be consistent with the gravel and sand particles using steel sieve sieving method. This manual sieving operation is adequate for testing a small amount of soil sample, but it becomes laborious and time-consuming when the amount of samples is large. Hence, there is a need to innovate a machine-based method for testing a large amount of soil samples.

The rotary vibrating sieve machine is an automated device for sieving and classifying particles and is used in mining, chemistry, food, environmental protection, and other fields [17]. Based on the motion type produced by the rotating vibrators, the sieving performance can have several types including unbalanced elliptical, balanced elliptical, circular, or linear [18,19]. In mining industries, the counter-rotating vibrating sieve with linear motion adopting the sieve with a minimum aperture of 0.095 mm can classify the tailings to improve the recovery of the concentrate and solve the plugging problem of fine coal in wet sieving [20]. In chemical industries, the plane sieve, rotary sieve, and vibrating sieve are combined for the anaerobic digestion separation by the sieve with a minimum aperture of 0.02 mm [21]. In food processing, the sieve with a rotary–reciprocating–oscillatory motion is applied for purifying oats to improve milling efficiency, and the sheet-metal sieve with a minimum aperture of 2 mm is used for dry sieving [22,23]. For environmental protection, the contaminated sites are treated using a high-frequency vibrating sieve with linear motion to remove heavy metals through washing and sieving, and the minimum aperture of the sieve is 0.1 mm [24].

In these studies, both dry sieving and wet sieving can be conducted by rotary vibrating sieve machines with different structures or different vibration motions, but the minimum sieve apertures of used sieves are all larger than 0.02 mm. In addition, there is no open literature (both Chinese and English) that has published similar research work on using this machine to wash and sieve silt and clay particles out from soils. Therefore, this study modifies the rotary vibrating sieve machine and redevelops it to conduct automatic washing and sieving operations. The steel and cloth sieves with different materials or different aperture sizes are replaced for soil washing and sieving.

1.4 Objective and outline

The objective of this study is to develop a machine-based washing and sieving method with a modified rotary vibrating sieve machine to separate silt and clay particles so that soil classification can be conducted accurately and efficiently. It is a technical improvement over the recently developed manual extended wet sieving approach [16,25].

In this study, the modified machine equipped with a steel sieve of aperture 0.063 mm is employed for separating gravel and sand particles from the soil. The modified machine equipped with cloth sieves with apertures from 0.048 to 0.0008 mm is introduced for separating silt and/or clay mixtures into individual groups of known particle size ranges. Based on the washing and sieving results, the classification of gravel and sand portions, silt and clay portions, and total soil particles are quantitatively determined. Furthermore, a comparative analysis between the machine-based method and the manual-based method is conducted from test duration, washing water, PSD result, and material mass loss rate. The dimensions of separate silt particles and clay particles are also analyzed with scanning electron microscopy (SEM) which verifies the effectiveness of the proposed machined-based washing and sieving method. This method can also be extended to the soil classification for different types of soil.

2 Rotary vibrating sieve machine and innovation

2.1 General

This machine-based washing and sieving method modifies the existing rotary vibrating sieve machine and conducts the washing and sieving operation for fine soils automatically. This machine consists of the frame portion (Fig. 1), the sieve portion (Figs. 2 and 3), and the power and electric portion (Fig. 4). In particular, the steel sieve of aperture 0.063 mm in the sieve portion is used for soil washing and sieving (Fig. 2). Additional cloth sieves with different apertures are placed flat on the upper surface of the steel sieve and fixed on the upper edge of the rotary vibrating sieve for washing and sieving mud slurry, silt slurry, and clay slurry (Fig. 3). The cloth sieve can be flexibly replaced according to the particle size of the materials. In addition, other auxiliary tools including a stainless-steel funnel and a hand-held electric mixer are used to assist the washing and sieving process (Fig. 5).

2.2 Frame portion of the rotary vibrating sieve machine

Figure 1 shows the frame portion consisting of 12 parts. The total height of this frame portion is 63 cm. The dustproof cover (No. 3) is 60 cm in diameter and 8 cm in height which plays a sealing role and can effectively dissipate dust. An inlet (No. 1) of 15 cm in diameter at the center of the dustproof cover is used for slurry feeding. To prevent the slurry from splashing out of the inlet during the sieving process, a silicone cover (No. 2) is used for sealing. The upper frame (No. 8) of 11 cm in height is used for containing the slurry retained on the sieve. The lower frame (No. 9) of 10 cm in height is used for containing the slurry passing through the sieve. These two frames are made of Q235 stainless steel with a thickness of 2 mm. Six semicircular clamp rings (No. 4) together with six clamp ring locks (No. 6) are used for fixing and sealing between the dustproof cover and the upper frame, between the upper frame and the lower frame, and between the lower frame and the baseplate (No. 10), respectively. To enhance the sealing performance and prevent the liquid from leaking out, three circular rubber sealing elements (No. 5) are installed inside the clamp rings, respectively. After completing the sieving process, the sealing baffle of the outlet on the upper frame can be opened and the coarse particles larger than the sieve aperture come out from this outlet (No. 7). This baffle ensures the fine particles can fully pass through the sieve apertures before the washing and sieving is completed. Fine particles which smaller than the sieve apertures will be washed out from the outlet (No. 7) located on the lower frame. The diameter of these two outlets is 11 cm. Nine springs (No. 11) are evenly set between the baseplate and the base (No. 12). These springs are primarily used for vibration absorption and noise control. The bottom of this cylindrical base has an

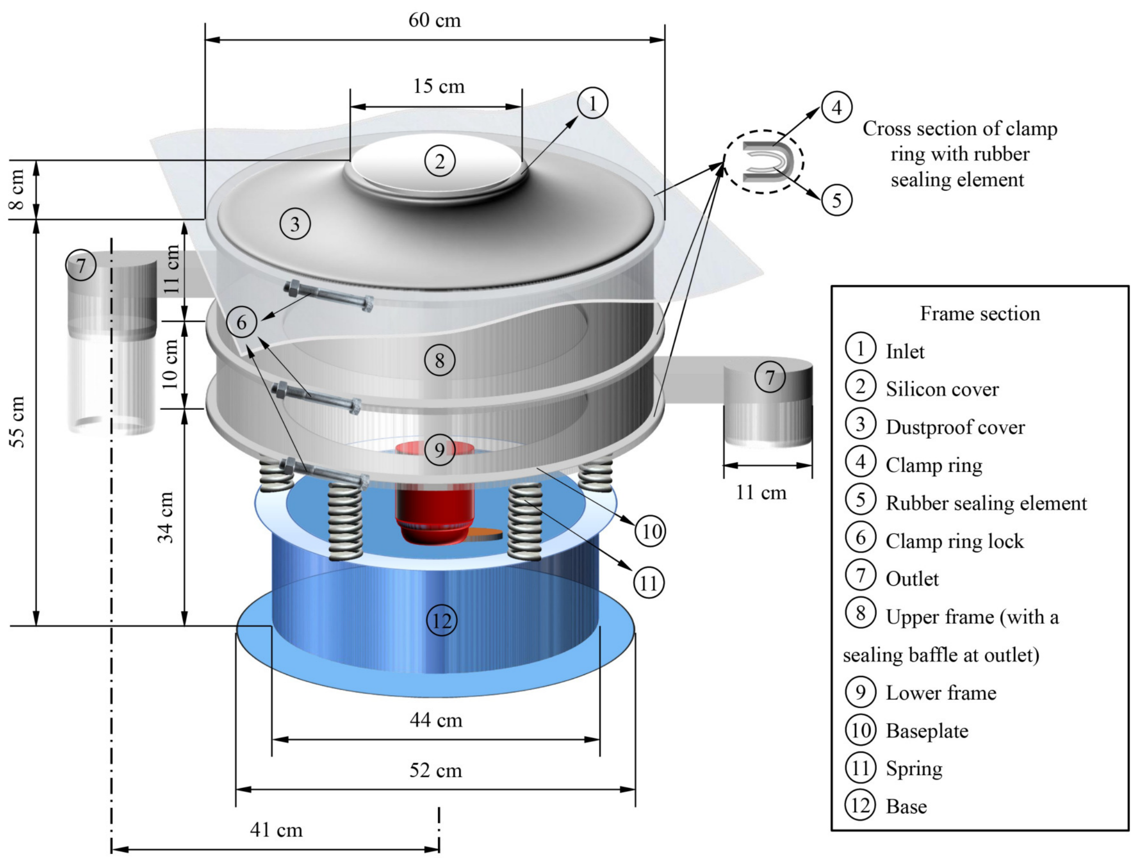

Fig. 1 Frame portion of rotary vibrating sieve machine.

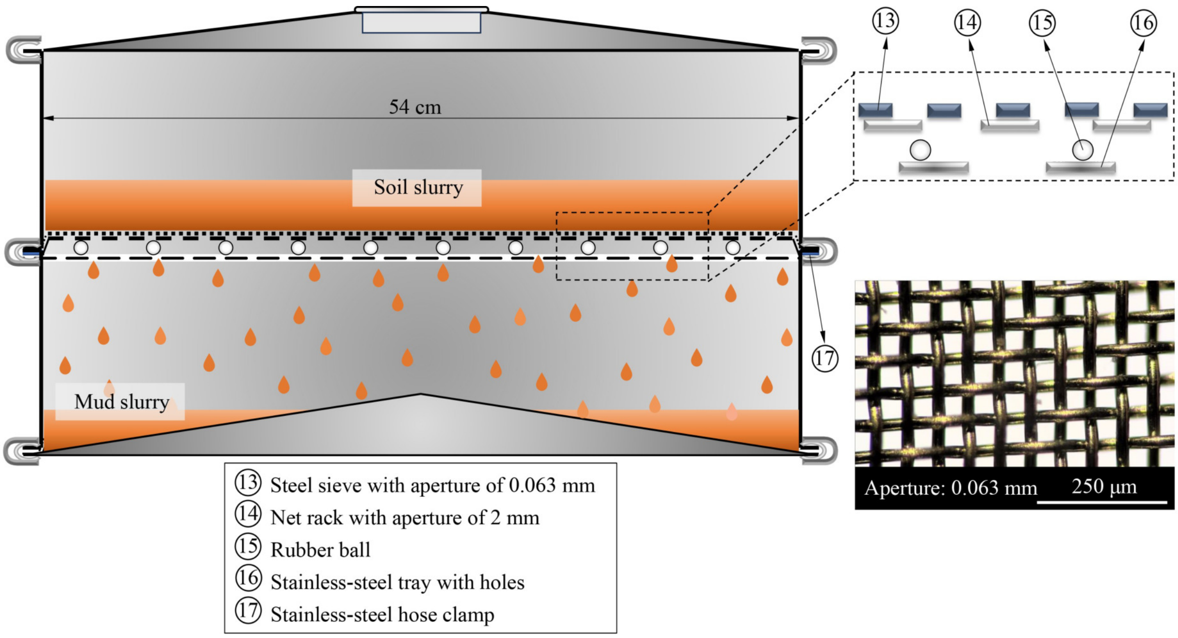

Fig. 2 Sieve portion with steel sieve layer of rotary vibrating sieve machine.

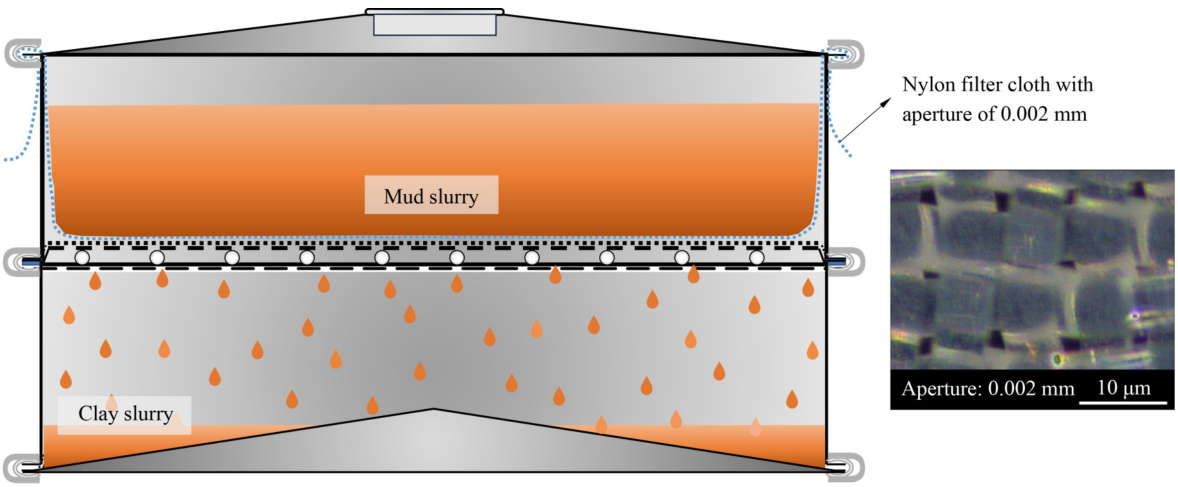

Fig. 3 Sieve portion with steel and cloth sieve layers of rotary vibrating sieve machine.

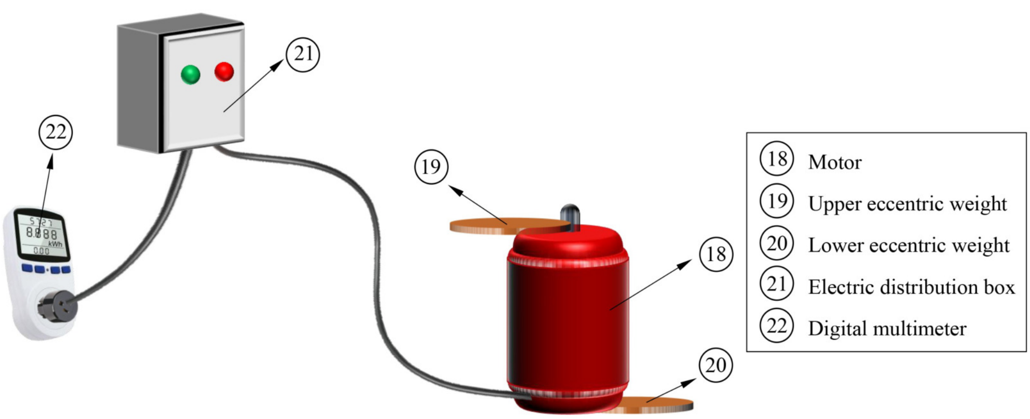

Fig. 4 Power and electric portion of rotary vibrating sieve machine.

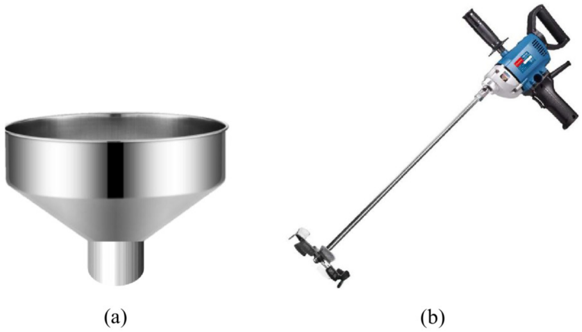

Fig. 5 Auxiliary tools: (a) stainless-steel funnel; (b) hand-held electric mixer.

inner diameter of 44 cm and an outer diameter of 52 cm. The vertical distance between the baseplate and the bottom of the base is 34 cm. The footprint of the whole frame portion is about 6793 cm^2.

2.3 Steel sieve portion of the rotary vibrating sieve machine for sand

Figure 2 shows the sieve portion between the upper frame and the lower frame. A 0.063 mm aperture is employed in the steel sieve to sieve soil slurry (No. 13). The material of the steel sieve is 304 stainless steel wire (Fig. 2). To avoid damage to the steel sieve due to the excessive pressure of the overlying slurry, the steel sieve is fastened on a circular net rack (No. 14) of aperture 2 mm with a stainless-steel hose clamp (No. 17). The steel sieve surface has a diameter of 54 cm and a sieving area of 2290 cm^2. Below the net rack, there is a stainless-steel tray with holes (No. 16) holding 15 rubber balls (No. 15). During the rotation and vibration of the machine, these rubber balls can collide with sieve layers constantly to avoid aperture blocking and improve the penetration of materials. The steel sieve, net rack, and stainless-steel tray are fastened and sealed with a rubber sealing element.

Since the reliability of the washing and sieving test results relies on the dimension of the sieve aperture, the size and shape of metal wire cloth apertures of a steel sieve should be calibrated regularly according to the method specified in ISO 3310-1 [26] and ASTM E11-26 [27].

2.4 Power and electric portion of the rotary vibrating sieve machine

Figure 4 illustrates the power and electric portion of the rotary vibrating sieve machine. The motor is an RCZL-8-4 vertical motor (No. 18). Two eccentric weights are installed at both ends of the motor (Nos. 19 and 20). This motor is set beneath the baseplate. The frequency and power of the motor are 1500 r/min and 0.66 kW, respectively, and this motor can generate an exciting force of 8 kN. The distribution box (No. 21) consists of a busbar, fuse links, switches, bypass equipment, and residual current detector. It can ensure the circuits are safe against short circuits. The working electricity is a three-phase voltage of 380 V, and its frequency is 50 Hz. The digital multimeter (No. 22) is used to measure the electricity consumption and the operation time of the machine.

2.5 Working principle of the rotary vibrating sieve machine

Jiang et al. [28] studied the structural characteristics and working principles of the rotary vibrating sieve. The vertical motor is used as the excitation source. The upper eccentric weight and lower eccentric weight convert the rotary motion of the motor into three-dimensional motion in horizontal, vertical, and inclined directions. The materials are mainly put in from the center of the round sieve surface. This three-dimensional motion is then transmitted to the sieve portion, and the materials move to the periphery along the spiral locus (Fig. 6). Compared with linear motion, this uniform circular motion avoids uneven stress concentration by rearranging the stress distribution on the sieve surface [18]. In addition, the materials will travel a longer distance on the sieve surface to make the washing and sieving more complete. The moving locus of the materials on the sieve surface can be changed by adjusting the phase angle of the upper and lower eccentric weights. At the same time, the materials on the sieve surface are bounced up and down which helps to thin and loosen the slurry. After the materials fall on the sieve, the fine materials smaller than the aperture size can pass through the sieve aperture, and discharge from the outlet of the lower frame. Finally, the mixed material is automatically divided into coarse particles and fine particles.

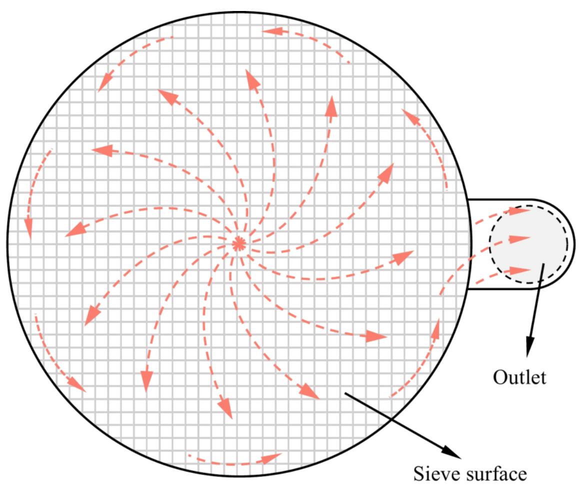

Fig. 6 Movement locus of soil particles on sieve surface.

2.6 Innovations of adding nylon cloth sieves for sieving silt and clay

The nylon filter cloth is used in industrial production and can be purchased from qualified stores online easily. The price of nylon filter cloth ranges from HK$ 10 to HK$ 270 per square meter with an aperture size of 0.048 to 0.0008 mm. The nylon filter cloth sieve has a smooth surface for the easy removal of silt and clay from the cloth surface [29]. The maximum heat-resistant temperature of this nylon filter cloth is from 80 to 120 °C. The tensile strength of this nylon filter cloth is from 50 to 95 MPa.

The nylon filter cloths of aperture size from 0.048 to 0.001 mm have been successfully applied for the manual wet sieving of silt and clay [16]. This manual sieving method took 705 min to separate 1588.8 g of dry silt and clay mixture into 8 sub-size groups of silt particles and 2 sub-size groups of clay particles. To meet the washing and sieving of a large quantity of soil, the efficiency of the previous manual wet sieving method needs to be improved. Considering that there has never been a precedent for combining this kind of nylon filter cloth and rotary vibrating sieve machine to work together for soil washing and sieving, the operability of this method and the particle size of final silt and clay particles need to be investigated and verified. As shown in Fig. 3, the nylon filter cloth is fixed on the upper edge of the upper frame of the rotary vibrating sieve with a rubber sealing element to form a cloth basket for washing and sieving. The 0.002 mm aperture is employed in the cloth sieve for sieving mud slurry (Fig. 3). The 0.048, 0.038, 0.014, 0.012, 0.0063, 0.004, and 0.003 mm apertures are employed in the cloth sieve for silt slurry washing and sieving. The 0.001 and 0.0008 mm are employed in the cloth sieve for clay slurry washing and sieving. The shape of the cloth sieve is a square with a side length of 1 m.

During laboratory testing, it is necessary to avoid scratching the nylon filter cloth on hard or sharp materials to damage the cloth. To ensure the repeatability of this washing and sieving process, the aperture sizes of the nylon filter cloth can be checked regularly using the same method as steel sieves. In addition, microscopic observation and micro-spherical glass sieving can also be used for calibrating the aperture size of each cloth sieve.

2.7 Other auxiliary tools

To improve the efficiency of washing and sieving and the convenience of operation, some auxiliary tools including a stainless-steel funnel and a hand-held electric mixer are necessary. The stainless-steel funnel (Fig. 5(a)) is used for slurry feeding and preventing slurry from leaking.

The hand-held electric mixer (Fig. 5(b)) is used for mixing and washing the soil with water before sieving with the rotary vibrating sieve. Due to the limitation of the natural disintegration of soil agglomerates in water, mechanical agitation can disperse the natural soil agglomerates into individual solid particles. The use of the hand-held electric mixer can improve the separation efficiency of individual particles and avoid large undispersed soil agglomerates damaging the sieve surface.

3 Machine-based washing and sieving method for soils

3.1 Soil material for testing

Volcanic rocks cover about 50% of Hong Kong (China)'s surface area [30]. The completely decomposed tuff (CDT) soil is a common *in situ* weathered soil from the complete chemical decomposition of volcanic rock in Hong Kong, China [31,32]. Acquired from a public housing building field in Wah King Street on Hong Kong Island (China), the CDT soil sample is utilized for washing and sieving. The parent rock of this CDT soil is eutaxitic fine ash vitric tuff and belongs to the Ap Lei Chau formation of Repulse Bay Volcanic Group [33]. Its specific gravity is 2.62 with a reddish-brown appearance color in nature.

3.2 Step I: Soil washing and sieving

At first, a total of 13.6 kg of dry CDT soil is placed into a bucket and mixed with water (Figs. 7(a) and 7(b)). The soil−water mixture in the bucket is mixed and stirred for a few minutes with the hand-held electric mixer (Fig. 7(c)). To maintain the natural state and the stability of the PSD result of soil, no dispersing agent is added throughout the test. The heavy and large gravel, sand, and some silt and clay particles sink to the bottom of the bucket. The soil slurry in the upper layer contains clay, silt, and fine sand particles. This soil slurry is subsequently poured into the rotary vibrating sieve machine with the steel sieve of aperture 0.063 mm for washing and sieving (Fig. 7(d)). Repeated washes for the large particles in the bucket are required with additional water until the soil slurry becomes clean. During the washing and sieving process, the outlet of the upper frame is closed with the baffle. The filtered mud slurry containing silt and clay mixture continuously discharges from the outlet of the lower frame (Fig. 7(e)).

When the mud slurry is drained, the dustproof cover is opened and new water to rinse the remaining materials on the steel sieve is added (Fig. 7(f)). This step is considered completed when the remaining materials on the sieve surface and the leachate are clean. The mud slurry flowing out from the outlet is contained in a bucket for further sieving in Step II (Fig. 7(g)). The mud slurry has a mass of 305.7 kg and a density of 1.0198 g/cm^3. Then, by opening the baffle of the outlet on the upper frame, the clean fine sand can come out of the outlet induced by the vibration of the machine. These clean fine sand particles are contained in a plate and mixed with the clean heavy and large particles (Fig. 7(h)) for further oven-drying and dry sieving. The gravel and sand portion has a dry mass of 4044.6 g, accounting for 30.22% of the dry CDT soil sample of 13.6 kg. Table 1 lists the results of this step. The time and electricity consumption of the machine in this step is 22 min and 0.078 kW·h, respectively.

3.3 Step II: Mud slurry washing and sieving

In Step II, the mud slurry from Step I is added to machine from the inlet with the assistance of a stainless-steel funnel (Fig. 8(a)). Then the inlet is sealed with a silicone cover and the machine is started for washing and sieving (Fig. 8(b)). Particles which smaller than 0.002 mm will seep out from the cloth sieve aperture due to the rotary vibrating force from the machine. As the washing and sieving progresses, more new water is added to dilute the dense mud slurry. This step is completed when the liquid flowing out from the outlet is clean or contains water only. The silt particles retained on the cloth sieve surface can be washed into a container with clean water after washing and sieving completion and removed from the machine.

Finally, the mass of the third portion of pinkish-brown silt slurry is 6042.6 g with a density of 1.6947 g/cm^3 (Fig. 8(c)). The mass of the fourth portion of reddish-brown

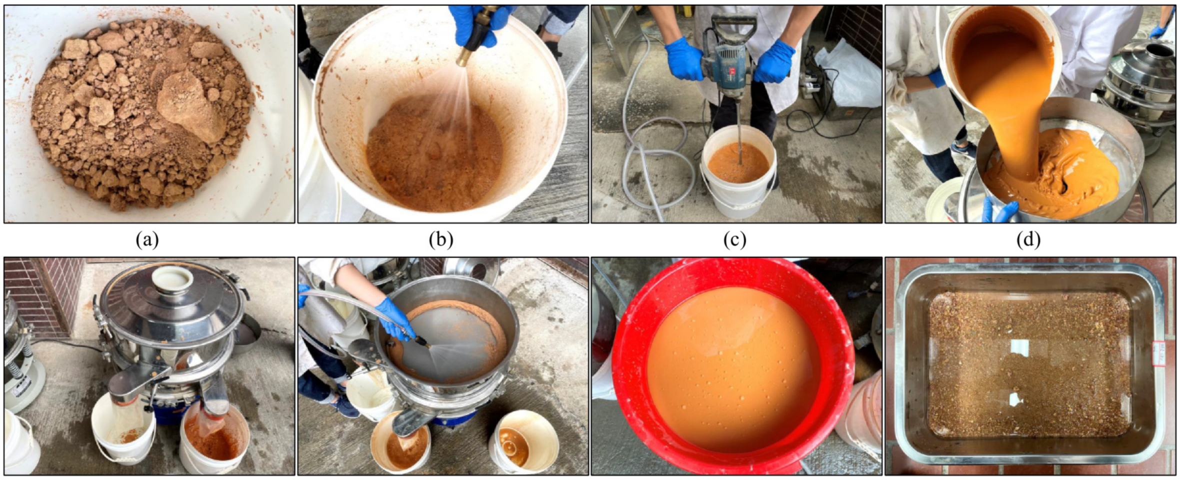

(a) (b) (c) (d) (e) (f) (g) (h)

Fig. 7 Process and results of soil washing and sieving: (a) CDT soil; (b) add water into a bucket; (c) stir with the hand-held electric mixer; (d) pour the soil slurry into the rotary vibrating sieve machine; (e) soil slurry washing and sieving; (f) wash fine sand with new clean water; (g) mud slurry; (h) clean gravel and sand mixture.

Table 1 Results of machine-based washing and sieving for 13.6 kg of CDT soil

Step	Aperture size (mm)	Mass of material a) to be sieved (kg)	Mass of added new water (kg)	Mass of material b) on the sieve (g)	Mass of material c) in the bucket (kg)	Test duration (min)	Electricity consumption (kW·h)
I	0.063	150.0	157.7	2000.0	305.7	22	0.078
II	0.002	305.7	69.3	6000.0	369.0	150	0.479
III	0.048	6.0	71.4	1148.1	76.3	9	0.027
	0.038	76.3	66.1	1881.2	140.5	17	0.058
	0.014	140.5	11.0	392.4	147.6	21	0.055
	0.012	147.6	19.3	1222.7	165.7	37	0.104
	0.0063	165.7	35.8	615.4	200.9	66	0.181
	0.004	200.9	9.2	394.1	209.7	30	0.104
	0.003	209.7	7.6	248.6	217.1	14	0.057
IV	0.001	369.0	118.6	833.4	486.8	181	0.514
	0.0008	486.8	60.2	3117.3	543.9	100	0.286

Notes: a) In Step I, the material is soil slurry; in Step II, the material is the second mud slurry; in Step III, the material is the first silt slurry; in Step IV, the material is the first clay slurry; b) in Step I, the material is the first gravel and sand; in Steps II, the material is the third silt slurry; in Step III, the material is the second silt slurry; in Step IV, the material is the second clay slurry; c) in Step I, the material is the second mud slurry; in Step II, the material is the fourth clay slurry; in Step III, the material is the third silt slurry; in Step IV, the material is the third clay slurry.

(a) (b) (c) (d)

Fig. 8 Process and results of mud slurry washing and sieving: (a) mud slurry feeding; (b) mud slurry washing and sieving; (c) the third portion of silt slurry; (d) the fourth portion of clay slurry.

clay slurry is 369 kg with a density of 1.0158 g/cm^3 (Fig. 8(d)). Table 1 shows the results of this step. The total time and total electricity consumption of the machine in this step are 150 min and 0.479 kW·h, respectively. These two portions of silt slurry and clay slurry will continue to do washing and sieving in the following Step III and Step IV, respectively.

3.4 Step III: Silt slurry washing and sieving

In Step III, the cloth sieve of 0.002 mm in aperture is substituted with the other seven cloth sieves with apertures of 0.048, 0.038, 0.014, 0.012, 0.0063, 0.004, and 0.003 mm accordingly. This washing and sieving operation for silt slurry is considered complete if the liquid flowing out of the outlet is clean. Table 1 shows the results of this step. The total time and total electricity consumption of the machine in this step are 194 min and 0.586 kW·h, respectively.

3.5 Step IV: Clay slurry washing and sieving

In Step IV, another two nylon cloths of aperture 0.001 and 0.0008 mm are used in turn for the fourth portion of clay slurry washing and sieving. The judgment basis for the end of this step is the same as that of Step III. Finally, the clay slurries in three sub-groups are then conducted static sedimentation for upper layer clean water separation and oven-drying. Table 1 shows the results of this step. The total time and total electricity consumption of the machine for this step are 281 min and 0.8 kW·h, respectively.

3.6 Washing water recycling from clay slurry

After static sedimentation, the resultant upper layer of water in the clay slurry is separated for purity testing using a UV-1900i UV-VIS Spectrophotometer. A total of seven 40 mL water samples from three groups (blank, experimental, and control) are tested. The blank group is the tap water. The experimental group contains three different water samples which are extracted from the clay slurry after one, two, and three hours of static sedimentation. The control group contains three uniquely synthesized water samples. These three water samples are prepared by manually adding 0.0001 g of coarse (0.002 to 0.001 mm), medium (0.001 to 0.0008 mm), and fine (< 0.0008 mm) clay particles with 40 mL of tap water.

Table 2 gives the list of complete experimental results. The spectrophotometer measures the absorbance value of tested water based on the principle that most compounds in water absorb light over different ranges of wavelengths. A lower absorbance value indicates a purer water, conversely, an opaque water will read an infinity absorbance value. Remarkably, the absorbance value for the water separated after static sedimentation for 1 h is the highest among the three experimental samples, which is 0.0015. This value is higher than that of the fresh tap water, but lower than that of the mixtures of 0.0001 g clay and 40 mL water. Consequently, it is inferred that the used water extracted from the slurry contains clay particles below 2.5 ppm, hence indicating its suitability for recycling and subsequent utilization in washing and sieving processes. After 24 h of static sedimentation, more than 85% of the water in the original clay slurry can be separated for recycling.

3.7 Used electricity and water for the washing and sieving test

From Steps I to IV, a total of 1.943 kW·h of electricity is consumed. In particular, Step I accounts for 4.01% of the total electricity consumption, but Steps II, III, and IV account for 24.65%, 30.16%, and 41.17% of the total electricity consumption, respectively. The electricity charge for non-residential electricity of Hong Kong (China) Electric Company Limited is HK$ 1.976 per unit (including basic charge and fuel clause charge). So, the total electric charge is HK$ 3.840. The electricity charges generated by the machine-based washing and sieving are listed in Table 3. The total machine operation time is 647 min. According to the research group's previous experiments, if the manual-based sieving method is adopted to complete the washing and sieving of the same particle size sequences within this time, only about 3 kg of soil can be completed.

In this study, about 0.77 m^3 of water is used from Steps I to IV. In particular, Step I accounts for 38.86% of the total washing water, and Steps II, III, and IV account for 9.09%, 28.75%, and 23.38% of the total washing water, respectively. According to the current water charge rate set by the Water Supplies Department of Hong Kong (China), the price of water for construction is HK$ 7.11 per cubic meter. So, the total water charge is about HK$ 5.47. The water charges generated by the machine-based washing and sieving are listed in Table 3. After static sedimentation for about 24 h, about 0.24, 0.042, 0.198, and 0.154 m^3 of water can be separated from slurry for recycling in Steps I, II, III, and IV, respectively. The total recycled water accounts for about 82% of the total washing water.

4 Results and classification of CDT soil

4.1 Result and classification of gravel and sand portion

The mechanical dry sieving process employs standard steel sieves with various aperture sizes, including 63, 14, 10, 6.3, 5, 3.35, 2.36, 2, 1.18, 0.6, 0.425, 0.3, 0.212, 0.15, 0.075, and 0.063 mm. These stereomicroscopic images of 15 distinct sub-groups of particles are presented in Fig. 9. These gravel and sand particles are all clean by visual inspection only and there are almost no silt or clay particles attached to the surface of them. This result reveals that tap water washing and sieving can separate soil into individual particles without a dispersing agent.

The distribution of particle sizes within the gravel and sand portion is expressed as Eq. (1):

$$PSD_{\text{gravel and sand portion}} = \frac{\sum_{j=11}^{M} W_{\text{b}j}}{W_{\text{total gravel and sand portion}}} \times 100\%, \quad (1)$$

Table 2 Results of purity testing of washing water recycled from clay slurry of 13.6 kg of CDT soil

Group	Material	Absorbance value
Blank group	40 mL tap water	0.0008
Experimental group	40 mL used water separated after static sedimentation for 1 h	0.0015
	40 mL used water separated after static sedimentation for 2 h	0.0011
	40 mL used water separated after static sedimentation for 3 h	0.0009
Control group	40 mL tap water + 0.0001 g clay (0.002–0.001 mm)	0.0019
	40 mL tap water + 0.0001 g clay (0.001–0.0008 mm)	0.0022
	40 mL tap water + 0.0001 g clay (< 0.0008 mm)	0.0026

Table 3 Used electricity and water results for washing and sieving 13.6 kg of CDT soil

Step	Duration (min)	Total electricity consumption (kW·h)	Electricity charge (HK$)	Total washing water (m^3)	Recycled water (m^3)	Water charge (HK$)
I	22	0.078	0.154	0.30	0.24	2.13
II	150	0.479	0.947	0.07	0.042	0.50
III	194	0.586	1.158	0.22	0.198	1.56
IV	281	0.800	1.581	0.18	0.154	1.28
Total	647	1.943	3.840	0.77	0.634	5.47

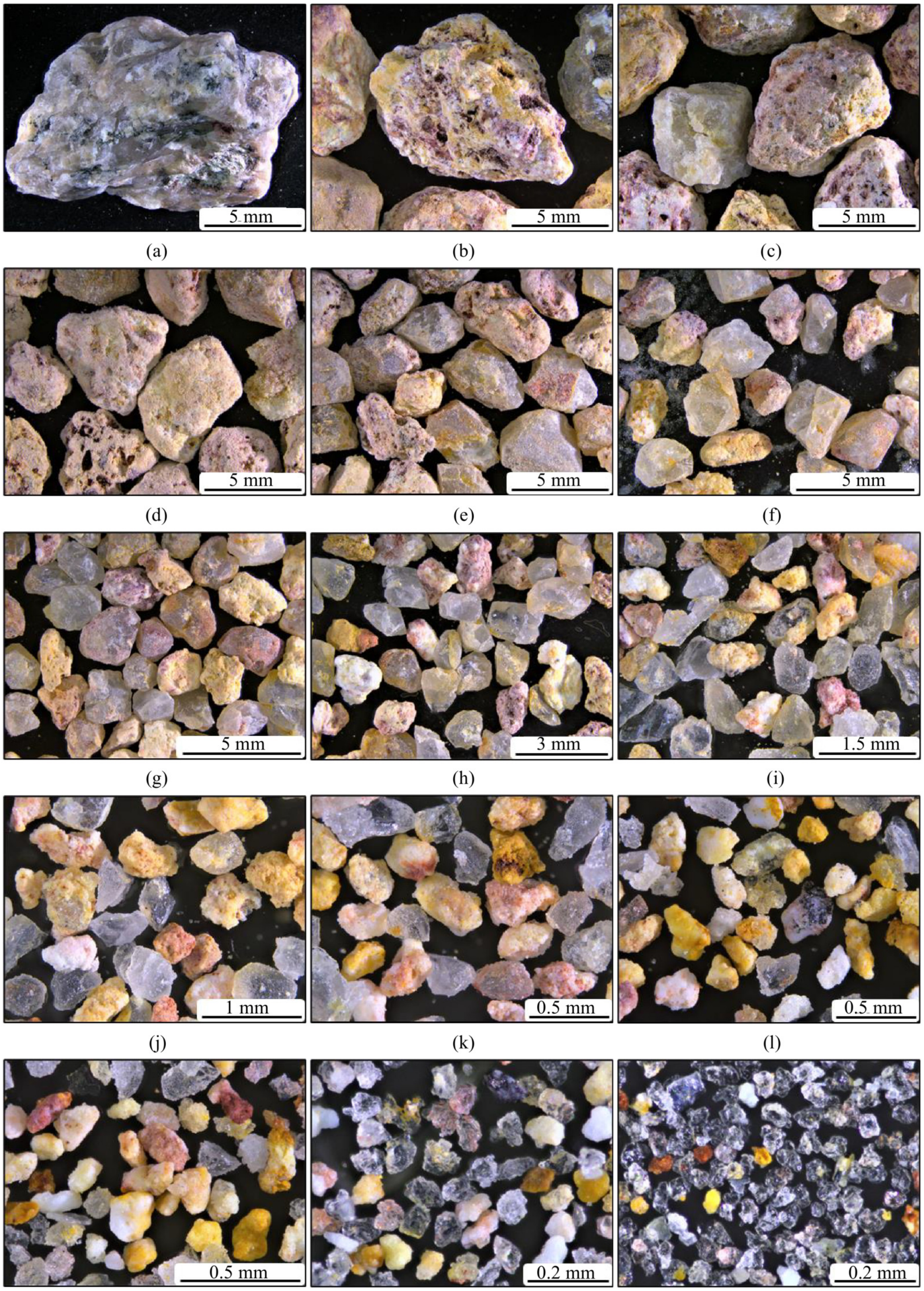

(a) (b) (c) (d) (e) (f) (g) (h) (i) (j) (k) (l) (m) (n) (o)

Fig. 9 Photos of gravel and sand in CDT soil after dry sieving: (a) 14–10 mm; (b) 10–6.3 mm; (c) 6.3–5 mm; (d) 5–3.35 mm; (e) 3.35–2.36; (f) 2.36–2 mm; (g) 2–1.18 mm; (h) 1.18–0.6 mm; (i) 0.6–0.425 mm; (j) 0.425–0.3 mm; (k) 0.3–0.212 mm; (l) 0.212–0.15 mm; (m) 0.15–0.075 mm; (n) 0.075–0.063 mm; (o) 0.063–0.048 mm.

where $PSD_{\text{gravel and sand portion}}$ represents the mass percentage finer than the Mth steel sieve aperture (M = 11,12,…,26); W_{bj} is the dry mass of the sand or gravel particles within the (j − 1)th and jth apertures (j = 11,12, …,26); and $W_{\text{total gravel and sand portion}} = \sum_{j=11}^{26} W_{bj}$. The jth aperture (j = 10,11,…,26) is 0.048, 0.063, …, 63 mm. The 10th sieve is the cloth sieve in Step III.

The PSD outcomes for the gravel and sand portion are given in Table 4 and Fig. 10. ISO 14688-1 (2018) classifies the particles with a size of 14 to 6.3 mm as medium gravel and the particles with a size of 6.3 to 2 mm as fine gravel. Similarly, the particles ranging from

2 to 0.63 mm, 0.63 to 0.2 mm, and 0.2 to 0.063 mm are classified as coarse sand, medium sand, and fine sand, respectively. The gravel particles account for 8.16% of the total mass, while the sand particles account for 91.02%. The curvature coefficient (C_c) and uniformity coefficient (C_u) of this PSD curve are 1.34 and 6.69, respectively. Consequently, based on the criteria outlined in ISO 14688-2 [34] and Geoguide 3 [5], the gravel and sand portion can be categorized as medium graded gravelly sand.

4.2 Result and classification of silt and clay portion

After static sedimentation and separating the upper clean water, the wet silt and highly saturated soft clay in each sub-group are put into the oven for drying. Figure 11 shows the stereomicroscopic images of 11 sub-size groups of silt and clay particles after drying. The silt portion consists of individual solid mineral particles. In the clay portion, the coarse clay and medium clay particles of sizing 0.002 to 0.0008 mm are mainly individual solid particles and contain some agglomerates composed of finer clay mineral particles. The fine clay particles of sizing less than 0.0008 mm are almost agglomerates of clay mineral particles.

The distribution of mass percentage within this portion is expressed as Eq. (2):

Table 4 PSD results of 13.6 kg of CDT soil

Particle category	Range[a)] (mm)	Mass (g)		$PSD_{\text{gravel and sand portion}}$ (%)	$PSD_{\text{silt and clay portion}}$ (%)	$PSD_{\text{CDT soil}}$ (%)
		Annotation	All			
Coarse to medium gravel	63–14	W_{b26}	0.0	100.00	100.00	100.00
Medium gravel-1	14–10	W_{b25}	1.6	99.96	100.00	99.99
Medium gravel-2	10–6.3	W_{b24}	8.1	99.76	100.00	99.93
Fine gravel-1	6.3–5	W_{b23}	14.8	99.39	100.00	99.82
Fine gravel-2	5–3.35	W_{b22}	94.6	97.06	100.00	99.11
Fine gravel-3	3.35–2.36	W_{b21}	207.8	91.92	100.00	97.56
Fine gravel-4	2.36–2	W_{b20}	3.1	91.84	100.00	97.53
Coarse sand-1	2–1.18	W_{b19}	768.3	72.85	100.00	91.79
Coarse sand-2	1.18–0.6	W_{b18}	1210.2	42.92	100.00	82.75
Medium sand-1	0.6–0.425	W_{b17}	444.7	31.93	100.00	79.43
Medium sand-2	0.425–0.3	W_{b16}	400.0	22.04	100.00	76.44
Medium sand-3	0.3–0.212	W_{b15}	200.6	17.08	100.00	74.94
Fine sand-1	0.212–0.15	W_{b14}	176.6	12.71	100.00	73.62
Fine sand-2	0.15–0.075	W_{b13}	452.1	1.54	100.00	70.24
Fine sand-3	0.075–0.063	W_{b12}	29.1	0.82	100.00	70.02
Coarse silt-1	0.063–0.048	W_{b11}	33.0	0.00	100.00	69.77
		W_{a11}	548.3	0.00	94.13	65.68
Coarse silt-2	0.048–0.038	W_{a10}	1085.7	0.00	82.50	57.57
Coarse to medium silt	0.038–0.014	W_{a9}	253.4	0.00	79.79	55.67
Medium silt-1	0.014–0.012	W_{a8}	788.2	0.00	71.35	49.78
Medium silt-2	0.012–0.0063	W_{a7}	311.4	0.00	68.01	47.46
Fine silt-1	0.0063–0.004	W_{a6}	155.4	0.00	66.35	46.30
Fine silt-2	0.004–0.003	W_{a5}	144.5	0.00	64.80	45.22
Fine silt-3	0.003–0.002	W_{a4}	691.4	0.00	57.40	40.05
Coarse clay	0.002–0.001	W_{a3}	337.1	0.00	53.79	37.53
Medium clay	0.001–0.0008	W_{a2}	1099.4	0.00	42.01	29.32
Fine clay	< 0.0008	W_{a1}	3923.2	0.00	0.00	0.00
Total particles	< 63	$W_{\text{CDT soil}}$	13382.6	100.00	100.00	100.00

Note: a) The particle size range of "63–14 mm" means "63 > particle size ⩾ 14 mm", the same as below.

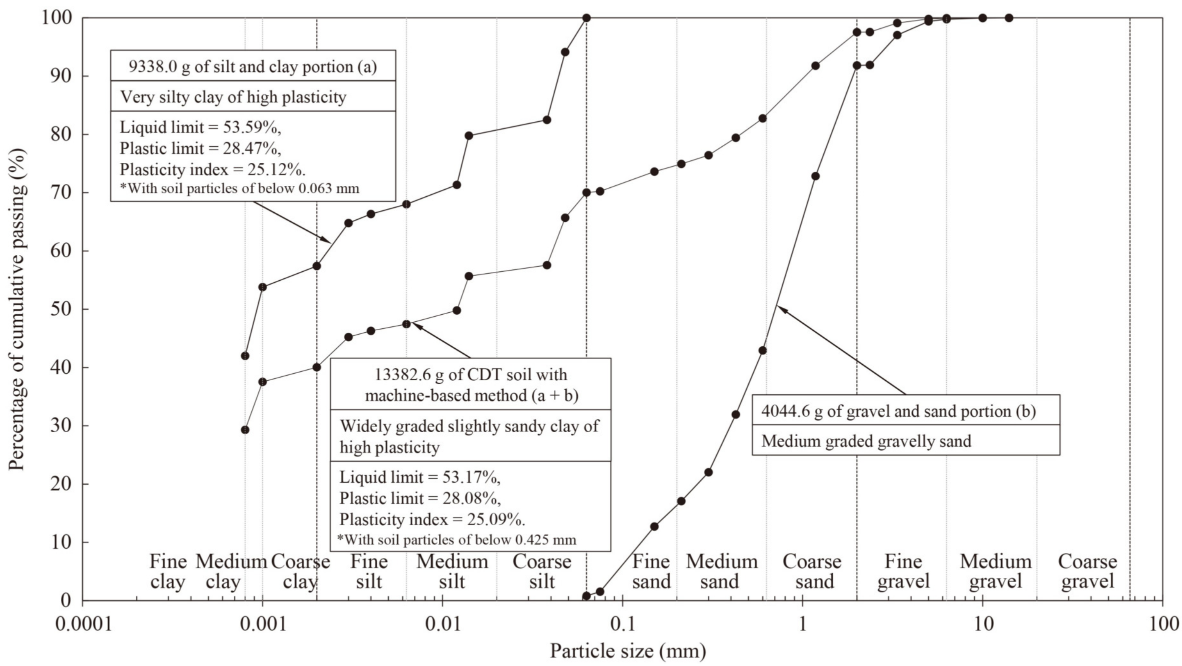

Fig. 10 PSD curves of 13.6 kg of CDT soil for classification.

$$PSD_{\text{silt and clay portion}} = \frac{\sum_{j=1}^{M} W_{aj}}{W_{\text{total silt and clay portion}}} \times 100\%, \quad (2)$$

where $PSD_{\text{silt and clay portion}}$ represents the mass percentage finer than the Mth cloth sieve aperture (M = 1,2,…,11); W_{aj} is the dry mass of the silt or clay particles within the (j − 1)th and jth apertures; and $W_{\text{total silt and clay portion}} = \sum_{j=1}^{11} W_{aj}$. The jth aperture (j = 0,1,2,…,10) is 0, 0.0008, 0.001, …, 0.048 mm.

Table 4 shows the PSD results of silt and clay portion. The PSD curve for the silt and clay portion is given in Fig. 10. The silt content and clay content are 42.60% and 57.40% of the silt and clay portion. ISO 14688-1 [14] classifies the particles with a particle size of 0.063 to 0.02 mm, a particle size of 0.02 to 0.0063 mm, and a particle size of 0.0063 to 0.002 mm as coarse silt, medium silt, and fine silt, respectively. Similarly, the other two particle sizes of 0.001 and 0.0008 mm divide clay particles into coarse clay, medium clay, and fine clay, respectively. The plasticity characteristics of soil particles below 0.063 mm are shown in Fig. 10. Therefore, the silt and clay portion can be categorized as very silty clay of high plasticity according to ISO 14688-2 [34] and Geoguide 3 [14].

4.3 Results and classification of total particles

The distribution of particle sizes of total particles is expressed using Eq. (3):

$$PSD_{\text{CDT soil}} = \frac{100\%}{W_{\text{CDT soil}}} \begin{cases} \left(\sum_{j=1}^{M} W_{aj}\right), \text{ for } 1 \leqslant M \leqslant 10, \\ \left(\sum_{j=1}^{11} W_{aj} + \sum_{j=11}^{M} W_{bj}\right), \text{ for } 11 \leqslant M \leqslant 26, \end{cases} \quad (3)$$

where PSD_{CDT} represents the mass percentage finer than the Mth sieve aperture; $W_{\text{CDT soil}} = W_{\text{total gravel and sand portion}} + W_{\text{total silt and clay portion}}$.

The final results of CDT soil can be found in both Table 4 and Fig. 10. The final total material mass is about 217.4 g less than the original dry CDT soil of 13.6 kg, and the mass loss rate is 1.6%. This loss can be caused by the few particles remaining in the equipment or leaking during the washing and sieving and dry sieving processes. The calculation and discussion of the material mass loss will be explained further in Subsection 5.3. The mass contribution within CDT soil is characterized by 2.47% gravel, 27.51% sand, 29.97% silt, and 40.05% clay. The plasticity characteristics of this CDT soil are shown in Fig. 10. According to the criteria of ISO 14688-2 [34] and Geoguide 3 [14], this CDT soil is denoted as widely graded slightly sandy clay of high plasticity.

5 Comparisons between machine and manual based washing and sieving methods

5.1 Comparison of test duration and washing water

To better compare this machine-based sieving method

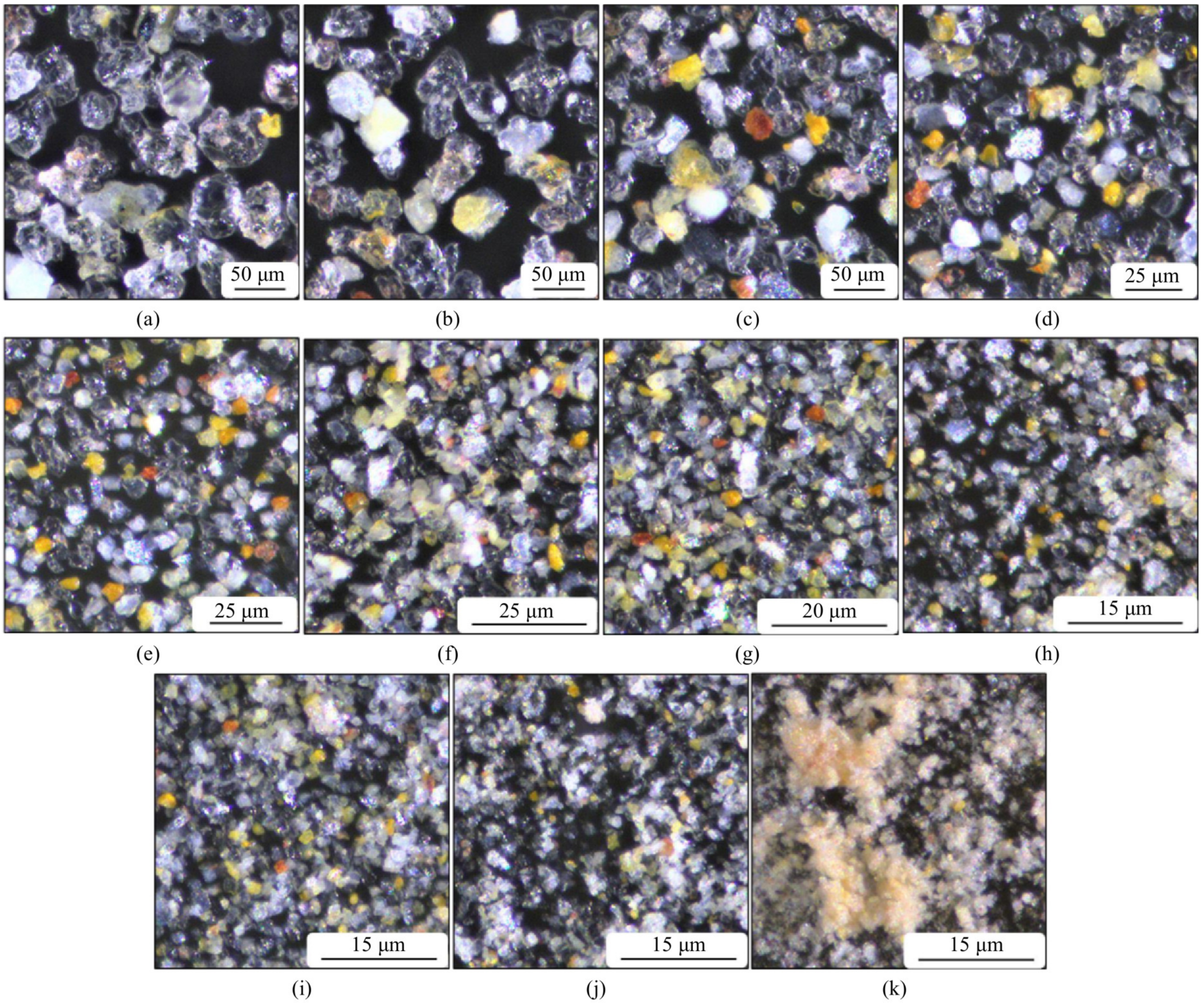

Fig. 11 Photos of silt and clay in CDT soil after drying: (a) 0.063–0.048 mm; (b) 0.048–0.038 mm; (c) 0.038–0.014 mm; (d) 0.014–0.012 mm; (e) 0.012–0.0063 mm; (f) 0.0063–0.004 mm; (g) 0.004–0.003 mm; (h) 0.003–0.002 mm; (i) 0.002–0.001 mm; (j) 0.001–0.0008 mm; (k) < 0.0008 mm.

with the manual-based sieving method intuitively, 1 kg of dry CDT soil is used for testing with these two methods, respectively. For the manual-based method, the steel sieve surface has a diameter of 30 cm and a sieving area of 706 cm^2. The size of the cloth sieve is the same as the machine-based method. The cloth sieve is tightened by a circular stretcher to form a sieve bag. The manual shaking and rotating frequency is about 120–150 r/min (equal to 2–2.5 Hz). Table 5 shows the test duration and washing water in each sieving step.

For the machine-based method, the time of machine operation in four steps is 5, 24, 28, and 24 min, respectively. During the machine sieving process, in addition to the automatic sieving of the machine, it is necessary to manually install the steel sieve or cloth sieve and seal the cover of the machine before adding new slurry into the machine. When adding new slurry or clean water, manual operation is necessary to stop the machine and feed new slurry or water. After the machine sieving is completed, the materials on the sieve need to be removed by rinsing with water and stored in desired containers. All of these processes require manual operations, and the time used is recorded as manual processing time. The manual processing time in four steps is 10, 15, 45, and 20 min, respectively. So, the total test duration for the machine-based method is 171 min. For the manual-based method, the manual shaking and rotating operation time in four steps is 30, 89, 52, and 167 min, respectively. During the manual sieving process, the manual processing time is consumed mainly by setting up steel sieve and cloth sieve and removing materials from the sieve to container. The manual processing time in four steps is 5, 5, 35, and 10 min respectively. So, the total test duration for the manual-based method is 393 min. Therefore, although the machine-based method still requires some manual processing, this method takes 222 min less than the manual-based method and is only 44% of the manual-based method.

As for washing water, the washing water used in the four steps of the manual-based method is 20, 10, 24, and 22 kg, respectively. The washing water used in the four steps of the machine-based method is 25, 5, 18, and

Table 5 Comparison of test duration and washing water for washing and sieving 1 kg of CDT soil using machine-based method and manual-based method

Step	Aperture size and manual processing time	Machine-based method		Manual-based method		Difference of two methods [a)]	
		Test duration (min)	Washing water (kg)	Test duration (min)	Washing water (kg)	Test duration (min)	Washing water (kg)
I	0.063 mm	5	25	30	20	−25	5
	Manual processing time	10	–	5	–	5	–
II	0.002 mm	24	5	89	10	−65	−5
	Manual processing time	15	–	5	–	10	–
III	0.048 mm	5	6	10	5	−5	1
	0.038 mm	5	3	10	5	−5	−2
	0.014 mm	4	2	8	3	−4	−1
	0.012 mm	4	2	6	4	−2	−2
	0.0063 mm	4	2	7	3	−3	−1
	0.004 mm	3	2	6	2	−3	0
	0.003 mm	3	1	5	2	−2	−1
	Manual processing time	45	–	35	–	10	–
IV	0.001 mm	15	12	82	12	−67	0
	0.0008 mm	9	10	85	10	−76	0
	Manual processing time	20	–	10	–	10	–
Total	–	171	70	393	76	−222	−6

Note: a) The difference in the test duration and washing water is calculated by subtracting the value of the manual-based method from the value of the machine-based method.

22 kg, respectively. So, the washing water used in each washing and sieving step between these two methods is similar.

5.2 Comparison of particle size distributions

Table 6 shows the final PSD results of these two methods. The mass of soil particles in each particle size obtained by the two methods is slightly different, which may be related to the difference in sampling. Figure 12 shows the PSD curves of 1 kg of CDT soil using machine-based method and manual-based method. The PSD results of silt and clay portion, gravel and sand portion, and all particles of these two methods are very close, and it shows that the machine-based method can obtain the same results as the manual-based method in a shorter time.

5.3 Comparison of soil mass loss rates

The sieving mass loss is the difference between the total mass of materials put on the sieve and the sum of all sieved fraction masses. In this machine-based method, the sieving mass loss can occur in washing and sieving process and dry sieving process. This loss is mainly from sieving blinding and attachment of fine particles to the sieve surface [35].

The mass loss rate of dry sieving, L_{dry}, is calculated using Eq. (4).

$$L_{\mathrm{dry}} = \frac{W'_{\text{total gravel and sand portion}} - W_{\text{total gravel and sand portion}}}{W'_{\text{total gravel and sand portion}}} \times 100\%, \tag{4}$$

where $W'_{\text{total gravel and sand portion}}$ is the dry mass of total gravel and sand portion before dry sieving.

The mass loss rate of washing and sieving, L_{wet}, is calculated using Eq. (5).

$$L_{\mathrm{wet}} = \frac{W'_{\text{CDT soil}} - (W'_{\text{total gravel and sand portion}} + W_{\text{total silt and clay portion}})}{W'_{\text{CDT soil}}} \times 100\%, \tag{5}$$

where $W'_{\text{CDT soil}}$ is the dry mass of soil sample before washing and sieving.

The total mass loss rate including washing and sieving and dry sieving, L_{total}, is calculated using Eq. (6).

$$L_{\mathrm{total}} = \frac{W'_{\text{CDT soil}} - W_{\text{CDT soil}}}{W'_{\text{CDT soil}}} \times 100\%. \tag{6}$$

Table 7 shows the calculation results of mass loss rates in gravel and sand dry sieving, CDT soil washing and sieving, and the whole process for machine-based method and manual-based method. The dry sieving mass loss rates between the two methods are the same (differ by 0.01% only) due to the identical dry sieving operation processes. As for the mass loss rates of washing and sieving, the value of machine-based method is 0.28%

Table 6 Comparison of PSD results for 1 kg of CDT soil using machine-based method and manual-based method

Particle category	Range (mm)	Machine-based method		Manual-based method		Difference of mass a) (g)
		Mass (g)	*PSD* (%)	Mass (g)	*PSD* (%)	
Coarse to medium gravel	63–14	0.0	100.00	0.0	100.00	0.0
Medium gravel-1	14–10	2.7	99.73	2.6	99.74	0.1
Medium gravel-2	10–6.3	2.5	99.47	2.7	99.47	−0.2
Fine gravel-1	6.3–5	1.9	99.28	1.8	99.28	0.1
Fine gravel-2	5–3.35	3.7	98.91	8.4	98.44	−4.7
Fine gravel-3	3.35–2.36	9.5	97.95	13.5	97.07	−4.0
Fine gravel-4	2.36–2	0.5	97.89	0.3	97.04	0.2
Coarse sand-1	2–1.18	39.1	93.94	45.6	92.44	−6.5
Coarse sand-2	1.18–0.6	65.5	87.31	79.5	84.42	−14.0
Medium sand-1	0.6–0.425	27.2	84.55	32.1	81.18	−4.9
Medium sand-2	0.425–0.3	25.1	82.01	31.8	77.97	−6.7
Medium sand-3	0.3–0.212	13.0	80.70	16.5	76.30	−3.5
Fine sand-1	0.212–0.15	10.7	79.61	13.5	74.94	−2.8
Fine sand-2	0.15–0.075	34.8	76.09	31.2	71.79	3.6
Fine sand-3	0.075–0.063	11.3	74.95	5.7	71.22	5.6
Coarse silt-1	0.063–0.048	36.5	71.25	36.3	67.55	0.2
Coarse silt-2	0.048–0.038	69.0	64.27	67.5	60.74	1.5
Coarse to medium silt	0.038–0.014	16.6	62.59	16.3	59.10	0.3
Medium silt-1	0.014–0.012	50.6	57.47	49.5	54.10	1.1
Medium silt-2	0.012–0.0063	20.4	55.40	18.6	52.23	1.8
Fine silt-1	0.0063–0.004	10.2	54.37	10.0	51.22	0.2
Fine silt-2	0.004–0.003	9.5	53.41	9.3	50.28	0.2
Fine silt-3	0.003–0.002	45.2	48.83	44.4	45.80	0.8
Coarse clay	0.002–0.001	31.6	45.63	29.2	42.85	2.4
Medium clay	0.001–0.0008	99.8	35.53	95.1	33.25	4.7
Fine clay	< 0.0008	351.0	0.00	329.5	0.00	21.5
Total particles	< 63	987.9	–	990.9	–	−3.0

Note: a) The difference in the mass of each sub-group material is calculated by subtracting the value of the manual-based method from the value of the machine-based method.

higher than that of manual-based method since a small amount of soil particles can remain in the nooks and crannies inside the machine. Overall, the total loss rate of the machine-based method is 0.3% higher than that of the manual-based method. In the future, the loss rate can be further reduced by improving the machine structure and optimizing the operating procedures.

6 Verifications for particle sizes of silt and clay

6.1 SEM examination and results

SEM image analysis is one of the methods to verify the machine-based washing and sieving results. The images of the 11 subcategories of silt to clay particles are acquired using a Hitachi S-3400N SEM. The silt and clay particles are all the samples after oven-dried at 105 to 110 °C. To facilitate analysis, the dry loose silt powder and dry clay after ground to pass a 0.063 mm test sieve within each sub-group are affixed to a sample stub with a diameter of 12.5 mm. Then the particles are coated with a layer of Au–Pd material.

Figure 13 shows the 11 coated silt and clay samples. The prepared stubs are placed into the chamber of the SEM under vacuum conditions. After the observation parameters of the equipment are set, the images of the particles are observed by adjusting the appropriate magnification, focal distance, contrast, and brightness. Figures 14–16 show the SEM images of silt and clay particles. The images of silt and clay sizing from 0.063 to

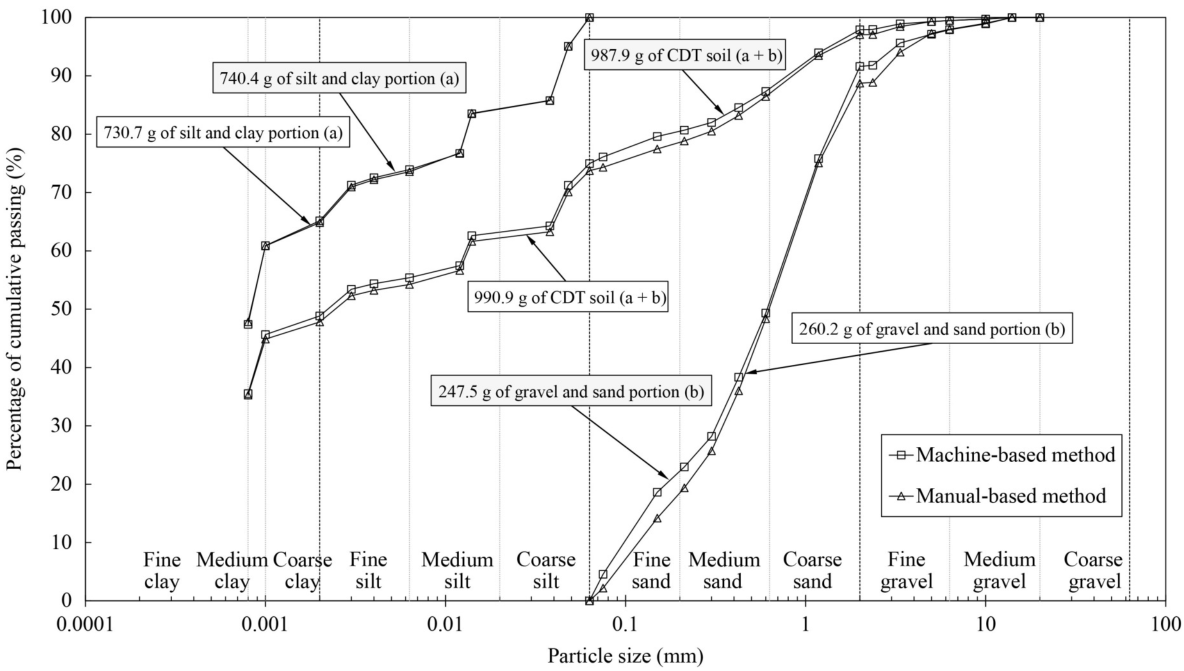

Fig. 12 Comparison of PSD results of 1 kg of CDT soil using machine-based method and manual-based method.

Table 7 Comparison of material mass loss rate for 1 kg of CDT soil using machine-based method and manual-based method

Item	Unit	Machine-based method	Manual-based method	Difference of two methods [a)]
Dry mass of soil sample before washing and sieving, $W'_{\text{CDT soil}}$	g	1000.0	1000.0	0.0
Dry mass of total gravel and sand portion before dry sieving, $W'_{\text{total gravel and sand portion}}$	g	249.8	262.3	−12.5
Mass of total gravel and sand portion after dry sieving, $W_{\text{total gravel and sand portion}}$	g	249.5	262.0	−12.5
Dry mass of total silt and clay portion, $W_{\text{total silt and clay portion}}$	g	740.4	730.7	9.7
Dry mass of CDT soil after washing and sieving and dry sieving, $W_{\text{CDT soil}}$	g	987.9	990.9	−3
Mass loss rate of dry sieving, L_{dry}	%	0.12	0.11	0.01
Mass loss rate of washing and sieving, L_{wet}	%	0.98	0.70	0.28
Total mass loss rate including washing and sieving and dry sieving, L_{total}	%	1.21	0.91	0.3

Note: a) The difference in the mass or loss rate is calculated by subtracting the value of the manual-based method from the value of the machine-based method.

0.0008 mm contain about 30 to 50 particles. Since the fine clay particles are very tiny, about 20 particles in a certain fine clay aggregate are selected for measurement. The SEM images are not used for gravel and sand particle analysis.

The SEM images in Figs. 14 and 15 reveal the granular nature of the silt particles, comprising discrete grains. Notably, these silt particles can be perceived as a natural extension derived from fine sand particles. The SEM images of the 3 sub-groups of clay with particle size below 0.002 mm are shown in Fig. 16. Figure 16(a) showcases individual mineral solid grains, which serve as an extension of the fine silt particles. In Fig. 16(b), the composition primarily comprises individual solid mineral particles, alongside a few particle agglomerates. Conversely, Fig. 16(c) is solely constituted of particle agglomerates. It is worth emphasizing that these clay particles in agglomerates have two shapes including a flat-like shape outlined with blue contour and a fiber-like shape outlined with green contour.

6.2 Digital image analysis of particle dimensions

The digital image analysis of individual particles is performed using ImageJ [36]. Calculations are performed on each selected particle to ascertain its major length with red marking, and its minor length with yellow marking. Notably, these two measurements are oriented perpendicularly. A total of 369 individual silt particles (Nos. 1–301) captured in Figs. 14 and 15, as well as clay particles (Nos. 302–369) captured in Fig. 16, are selected for the digital image calculations. As mentioned above, the fine clay particles have two particle shapes (Fig. 16(c)), which are divided into flat shape sub-group (Nos. 350–359) and fiber shape sub-group (Nos. 360–369). The measurement results are presented in Fig. 17.

Fig. 13 Eleven coated silt and clay samples used for SEM observation.

The establishment of upper and lower thresholds for individual sub-groups relies on the aperture size chosen for the cloth sieve implemented in the washing and sieving process. Figure 17(a) illustrates that the majority of major lengths observed in both silt and clay particles surpass the upper limit established for each respective sub-group. Figure 17(b) reveals that almost all observed minor lengths fall below the upper limit while exceeding the lower limit for each respective sub-group. Notably, within the coarse silt-1, coarse silt-2, and medium silt-1 sub-groups, a few minor lengths are below their lower limits. In the coarse to medium silt and fine silt-2 sub-groups, some minor lengths exceed the individual upper limits. These two phenomena can be caused by few smaller-sized silt particles without thorough washing and sieving, or few larger-sized silt particles remaining on the nylon cloth without thorough cleaning.

In summary, these findings reveal the significance of minor lengths in determining whether silt and clay particles can successfully pass through the cloth sieve aperture. This result is consistent with the particle size definition for standard steel sieve sieving method for gravel and sand [7,8,15].

The minor length to major length ratio serves as a representative measure of the shape characteristics of individual silt and clay particles (Fig. 17(c)). To further investigate this, Table 8 provides the minimum, maximum, median, mean, standard deviation, and coefficient of variation values for the minor/major ratios of selected particles. These findings indicate that the silt particles exhibit a nearly equal dimensional shape. Interestingly, the coarse clay and medium clay particles demonstrate statistical results similar to those of the silt particles, suggesting that most particles within the size range of 0.002–0.0008 mm could be considered as an extension of the silt particles. However, the fine clay particles which smaller than 0.0008 mm exhibit a high coefficient of variation. This phenomenon is attributed to the presence of fiber-shaped clay particles that possess smaller minor/major ratio in comparison to flat-shaped clay particles.

6.3 Critical size between silt and clay particles

Similar to fine sand particles, silt has a relatively high permeability and low plasticity. It behaves like flour when dry and becomes smooth and muddy when wet. Silt saturates quickly and has a viscous fluid-like characteristic [37]. By contrast, clay particles primarily originate from the chemical weathering of parent rock

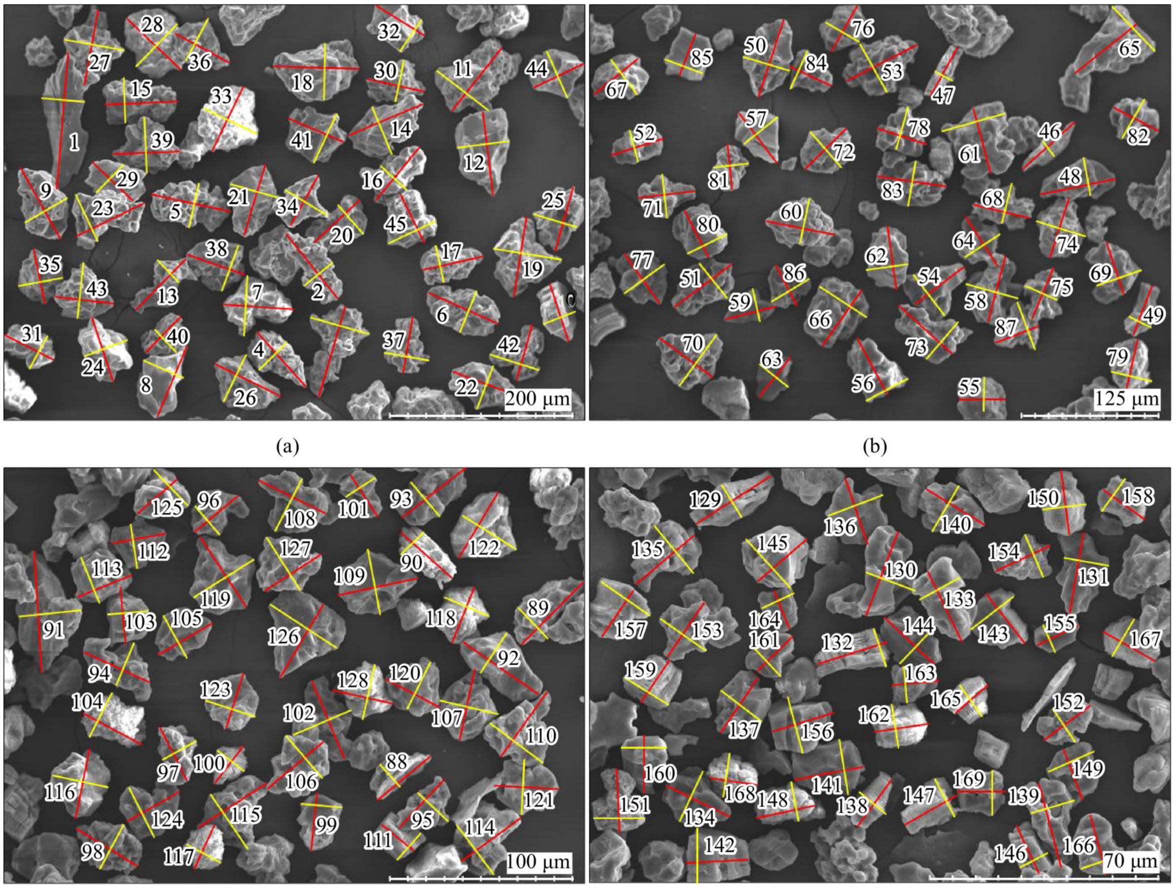

(a) (b) (c) (d)

Fig. 14 SEM images of coarse to medium silt particles: (a) 0.063–0.048 mm; (b) 0.048–0.038 mm; (c) 0.038–0.014 mm; (d) 0.014–0.012 mm.

and are characterized by thin, rigid structures with notable interparticle spaces, leading to their low permeability [38]. The minerals present in clay usually present a plate-like structure and comprise silica tetrahedron blocks and aluminum/magnesium octahedron blocks [39,40]. Therefore, there are significant differences between silt particles and clay particles in geometric, physical, and chemical properties. Accurately determining the critical size between silt and clay particles can help distinguish pure clay mineral particles from silt particles.

Upon examination of SEM images, the medium clay particles within the size range of 0.001–0.0008 mm mainly consist of discrete solid mineral grains and a few clustered clay mineral particles. Determining whether soil particles are aggregated or not can be judged by the overlapping and adhesion of the particles. These solid mineral grains have similar particle shapes to silt. Conversely, the fine clay particles comprise aggregated clusters characterized by flat-like and fiber-like structures. From particle size of 0.002 to those less than 0.0008 mm, the silt particles become less and less, and clay particles become more and more. This observation indicates that the size interface between silt and clay is not abrupt and is gradually changing from more to less silt particles and less to more clay particles. Hence, the size interface or threshold between silt and clay needs to be further quantitatively examined.

The chemical elements of 11 sub-groups of silt and clay are examined using energy-dispersive spectroscopy integrated with the SEM system. In the silt particles of size 0.048 to 0.038 mm, the weight percentages of eight main chemical elements (i.e., oxygen, silicon, magnesium, potassium, aluminum, calcium, sodium, and iron) are 61.59%, 35.48%, 0.00%, 0.07%, 1.40%, 0.00%, 0.00%, and 1.18%, respectively. This result indicates that the silt particles can mainly be the particles of quartz (i.e., SiO_2) and iron oxides with some particles of orthoclase feldspar (i.e., $KAlSi_3O_8$), plagioclase feldspar (i.e., $NaAlSi_3O_8$-$CaAl_2Si_2O_8$) and/or biotite (i.e., $K(Mg,Fe)_3(AlSi_3O_{10})(OH)_2$).

In the clay particles of size less than 0.0008 mm, the weight percentages of eight main chemical elements (i.e., oxygen, silicon, magnesium, potassium, aluminum, calcium, sodium, and iron) are 59.32%, 17.72%, 0.04%, 0.36%, 17.38%, 0.08%, 0.08%, and 4.55%, respectively. This result indicates that clay particles can mainly have the particles of clay minerals such as kaolinite (i.e.,

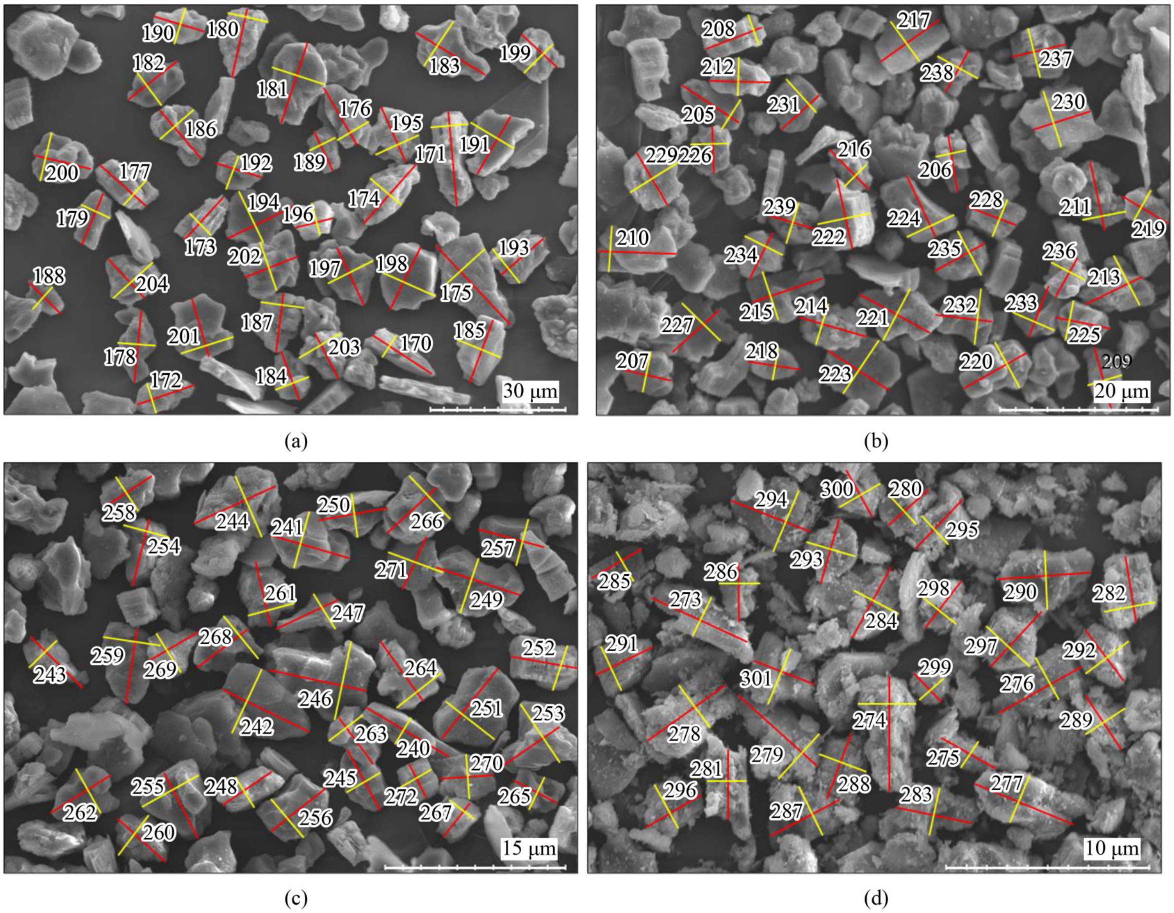

Fig. 15 SEM images of medium to fine silt particles: (a) 0.012–0.0063 mm; (b) 0.0063–0.004 mm; (c) 0.004–0.003 mm; (d) 0.003–0.002 mm.

$Al_2Si_2O_5(OH)_4$), and iron oxides.

6.4 Extension of the machine-based method to other types of soil

The machine-based washing and sieving method has been applied to 118 types of soils from 100 sites throughout China for soil classification. These 118 types of soils are briefly described as follows. 1) 7 types of desert soils from 4 sites in Xinjiang, and 3 sites in Inner Mongolia; 2) 11 types of loess soils from 1 site in Xinjiang, 5 sites in Shaanxi, 4 sites in Shanxi, and 1 site in Gansu; 3) 34 types of farmland soils from 1 site in Heilongjiang, 2 sites in Jilin, 9 sites in Inner Mongolia, 2 depths at 1 site in Beijing, 4 sites in Shandong, 1 site in Shanxi, 1 site in Chongqing, 5 depths at 3 sites in Sichuan, 1 site in Yunnan, 4 depths at 2 sites in Anhui, 2 depths at 1 site in Hunan, and 2 depths at 1 site in Hainan; 4) 26 types of completely decomposed granitic (CDG) or volcanic (CDV) soils from 3 sites in Shandong, 1 site in Fujian, and 22 sites in Hong Kong, China; 5) 25 types of slope soils of weathered sedimentary rocks from 1 site in Jilin, 1 site in Gansu, 9 sites in Qinghai, 1 site in Shanxi, 2 sites in Anhui, 1 site in Hunan, 3 sites in Yunnan, 2 depths at 1 site in Sichuan, 1 site in Chongqing, 1 site in Fujian, 1 site in Guangdong, and 2 depths at 1 site in Hainan; 6) 3 types of marine deposits from 3 sites in Hong Kong, China; 7) 10 types of soft soils from 10 depths at 1 site in Shanghai; 8) 2 types of public fill soils from 2 sites in Hong Kong, China.

The particles with sizes from gravel, sand, silt, and clay in these 118 soil samples are completely separated and verified. For example, the PSD curves of eight soil types with their GPS locations are shown in Fig. 18. They represent a loess soil from Lvliang in Shanxi, a marine deposit from Tung Chung in Hong Kong, China, a farmland soil from Harbin in Heilongjiang, a CDV soil from Tai Mo Shan in Hong Kong, China, a CDG soil from Happy Valley in Hong Kong, China, a slope soil from Changchun in Jilin, a public fill soil from Tuen Mun in Hong Kong, China, and a desert sand from Hami in Xinjiang, respectively. Their contents in weight for the particle sizes smaller than 0.002 mm (or clay) are 68.78%, 55.12%, 50.45%, 45.33%, 42.27%, 17.84%, 15.15%, and 0.59%, respectively. Other results and more analyses will be presented and examined in future publications.

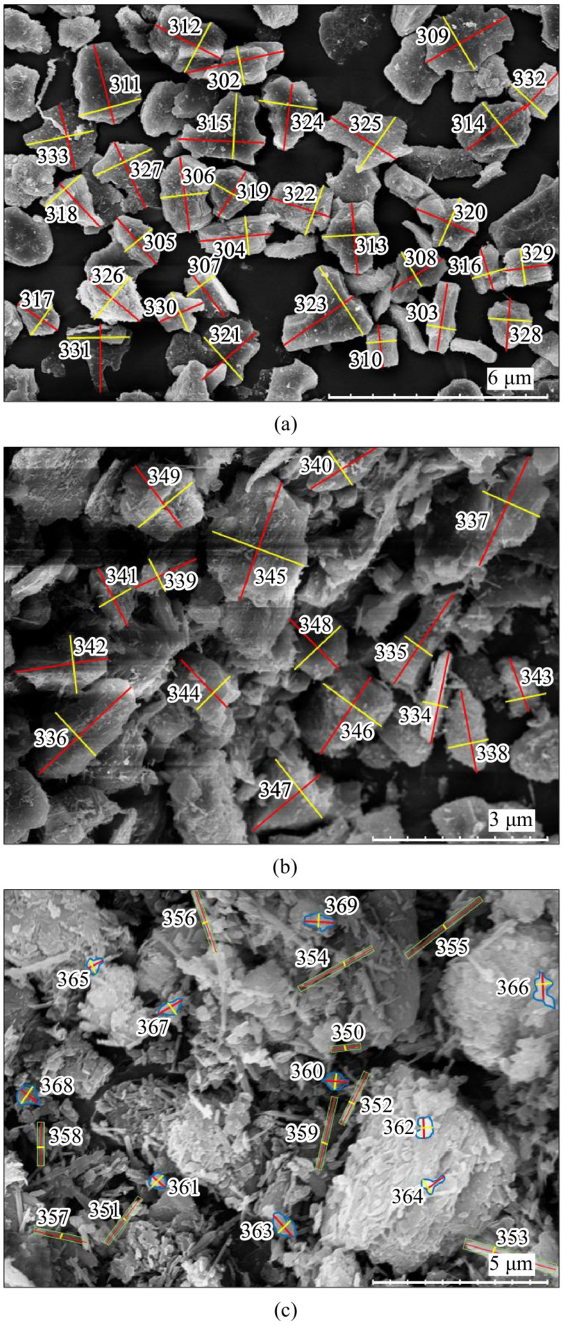

Fig. 16 SEM images of clay particles: (a) 0.002–0.001 mm; (b) 0.001–0.0008 mm; (c) < 0.0008 mm.

7 Conclusions

This paper develops a machine-based method for completely washing and sieving soils into gravel, sand, silt, and clay. It modifies and upgrades an existing rotary vibrating sieve machine by using the steel sieve of aperture size 0.063 mm and the nylon filter cloths of aperture sizes from 0.048 to 0.0008 mm for washing and sieving fine soils. The modification extends the aperture size limit of the existing rotary vibrating sieve machine to 0.0008 mm for separating silt and clay mixture into many sub-groups of silt and clay particles. Test results have shown that the machine-based method can greatly shorten the test time and generate accurate results for silt and clay particles according to the cloth sieve aperture sizes. Hence, the classification of gravel and sand portion, silt and clay portion, and CDT soil can be accurately and physically determined based on the result of complete PSD. The dimensions of separated silt and clay particles are further quantitatively verified with SEM image analysis. The machine-based washing and sieving method has been applied to 118 types of soils from 100 sites throughout China for soil classification. The proposed machine-based washing and sieving method conveniently and effectively separates different types of soils into gravel, sand, silt, and clay materials of different given particle sizes, thereby independently verifying the results and accurately classifying different types of soils. The main findings are concluded as follows.

1) The modified rotary vibrating sieve machine employs nylon filter cloths of very small aperture sizes from 0.048 to 0.0008 mm for silt and clay washing and sieving. The newly added cloth sieve can work well with the machine to accurately separate the silt and clay into their particles of various sizes. The gravel, sand, silt, and clay particles after washing and sieving are all clean by visual inspection and size well-defined, which indicates that the tap water washing can separate soil into individual particles without dispersing agent. The cleanness of the particles is to be examined with dispersing method in the future publication. The quantitative analysis of the impact of huge amounts of water rinsing and mechanical disturbance on the physical state of soil particles will also be studied further in the future. This machine-based method extends the manual-based method and improves the efficiency greatly without loss of accuracy.

2) The soil classification of the CDT soil is carried out by evaluating the complete and continuous PSD, as well as the plasticity of soil particles of certain particle size ranges. This complete mass-based PSD from gravel to clay improves the existing soil classification methods. This CDT soil is categorized as widely graded slightly sandy clay of high plasticity.

3) The water from clay slurry used in the separation process can exhibit a clay content below 2.5 ppm, which can be recycled or reused for the next round of the testing process. A total of 1.943 kW·h of electricity and 0.77 m^3 of water are used to complete the entire machine-based washing and sieving process for 13.6 kg of dry CDT soil. More than 85% of the water in original clay slurry can separated for recycling after 24 h static sedimentation.

4) According to the test results of 1 kg soil sample, the difference between material mass loss rates of the machine-based method and the manual-based method is very small, and the test duration of machine-based

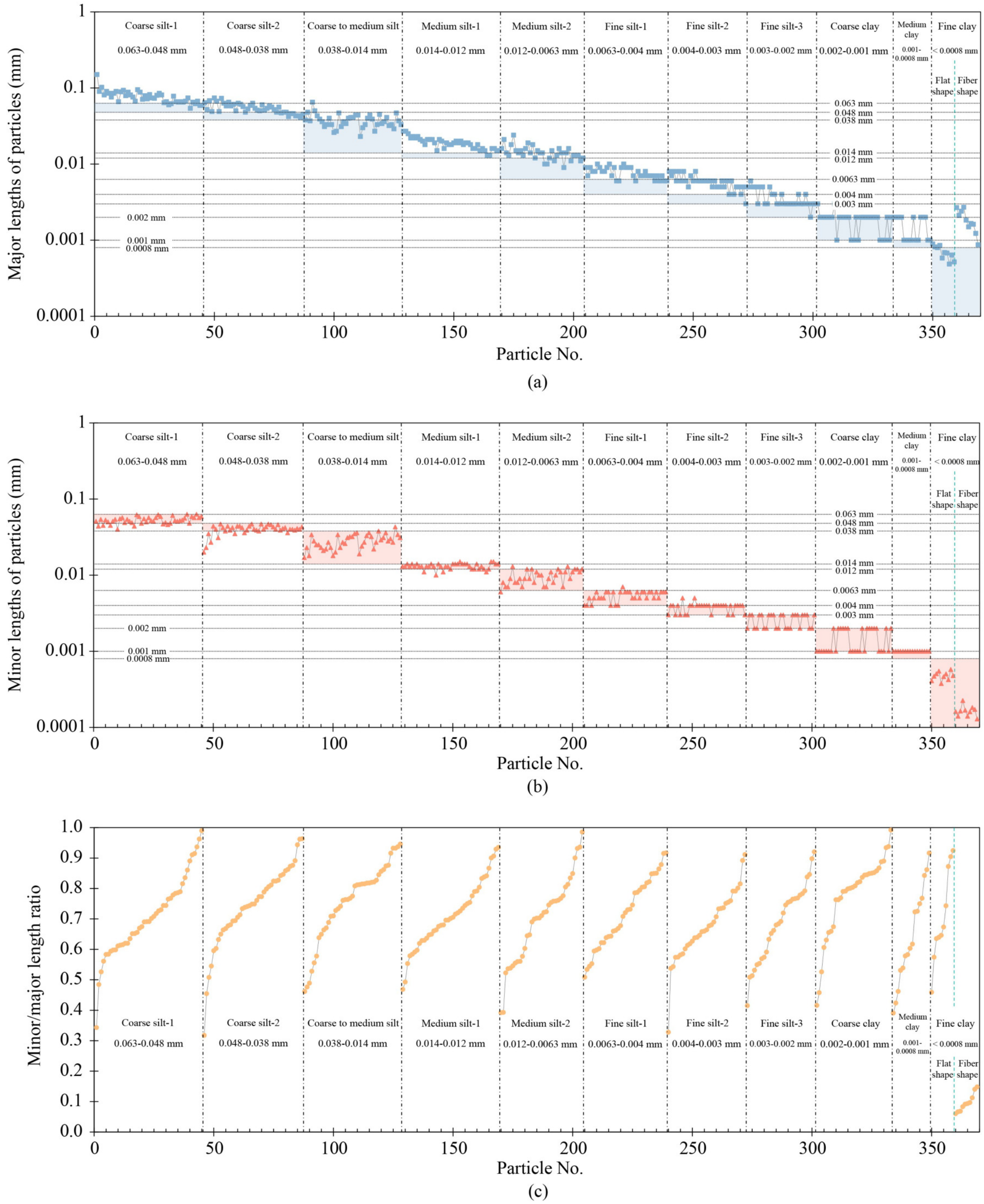

Fig. 17 Quantitative assessment for silt and clay dimensions: (a) major length of silt and clay particles; (b) minor length of silt and clay particles; (c) ratio of minor length of particles to minor length of particles.

Table 8 Statistical analysis of minor/major ratios of silt and clay particles from 13.6 kg of CDT soil

Particle category	Minimum	Maximum	Medium	Mean	Standard deviation	Coefficient of variation
Coarse silt to fine silt	0.317	0.990	0.720	0.714	0.127	0.178
Coarse clay and medium clay	0.391	0.992	0.780	0.731	0.154	0.211
Fine clay	0.060	0.925	0.304	0.402	0.331	0.825

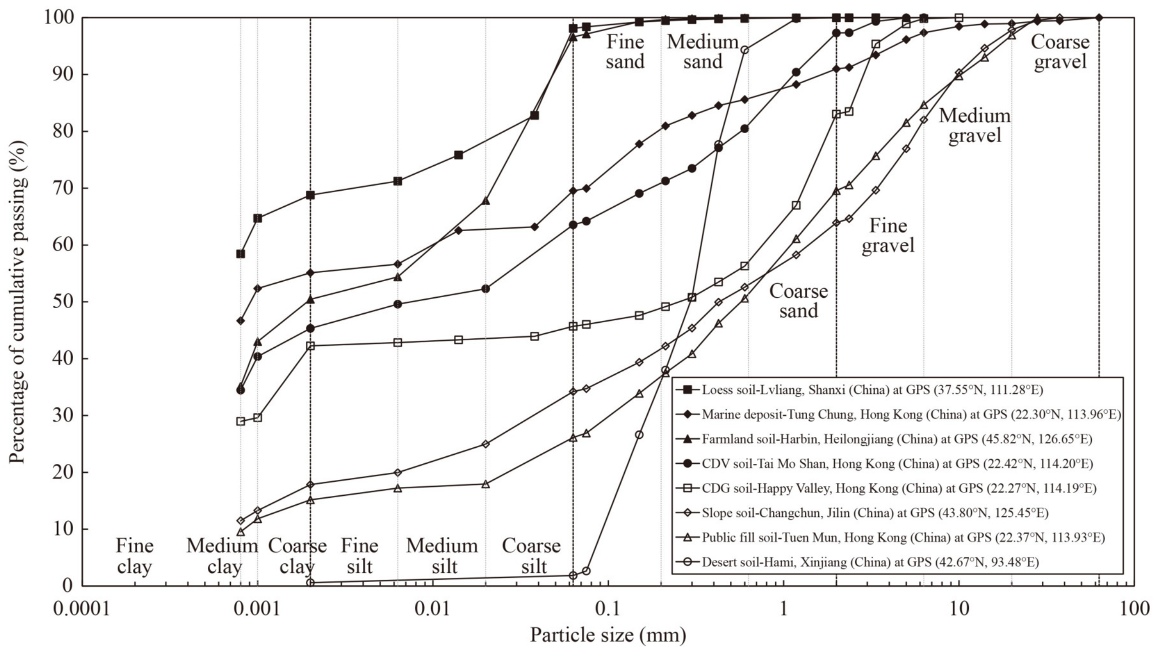

Fig. 18 PSD curves of 8 soil types determined with the proposed machine-based method and the soil GPS locations.

sieving can be greatly reduced. In this condition, both machine-based method and manual-based method are feasible. As the amount of soil increases, the manual-based method will consume a lot of manpower and time costs, and the time-saving and labor-saving characteristics of the machine-based method will become more prominent.

5) The results of SEM observation and image analysis reveal that the silt particles exhibit an equal-dimensional nature with sub-angular characteristics. Fine clay particles, displaying both flat-like and fiber-like shapes, are typically observed at sizes below 0.0008 mm. The critical threshold between silt and clay is not abrupt and is gradually changing from more to less silt particles and less to more clay particles.

Acknowledgements The authors acknowledge financial support provided by the Research Grant Council of the Hong Kong Special Administrative Region, China (Nos. HKU 17207518 and R5037-18).

References

1. Park J, Santamarina J C. Revised soil classification system for coarse-fine mixtures. Journal of Geotechnical and Geoenvironmental Engineering, 2017, 143(8): 04017039
2. Tiwari B, Ye G, Li M, Khalid U, Yadav S K. Strength and dilatancy behaviors of deep sands in Shanghai with a focus on grain size and shape effect. Journal of Rock Mechanics and Geotechnical Engineering, 2020, 12(6): 1214–1225
3. Guo Q, Zhan L, Shen Y, Wu L, Chen Y. Classification and quantification of excavated soil and construction sludge: A case study in Wenzhou, China. Frontiers of Structural and Civil Engineering, 2022, 16(2): 202–213
4. BS 5930. Code of Practice for Site Investigations. London: British Standard Institution, 1999
5. Geoguide 3. Guide to Rock and Soil Descriptions. Hong Kong (China): Civil Engineering and Development Department, 2017
6. ASTM D2487-17. Standard Practice for Classification of Soils for Engineering Purpose (Unified Soil Classification System). West Conshohocken: ASTM International, 2020.
7. ASTM D422-63. Standard Test Method for Particle-Size Analysis of Soils. West Conshohocken: ASTM International, 2007
8. BS 1377-2. Method of Test for Soils for Civil Engineering Purposes—Part 2: Classification Tests. London: British Standard Institution, 1990
9. Chepil W S. A compact rotary sieve and the importance of dry sieving in physical soil analysis. Soil Science Society of America Journal, 1962, 26(1): 4–6
10. Chapuis R P, Duhaime F, Weber S. Simplifying the calculation of equivalent diameter in sedimentation tests. Canadian Geotechnical Journal, 2015, 52(8): 1186–1189
11. Konert M, Vandenberghe J E F. Comparison of laser grain size analysis with pipette and sieve analysis: A solution for the underestimation of the clay fraction. Sedimentology, 1997, 44(3): 523–535
12. Lu N, Ristow G H, Likos W J. The accuracy of hydrometer analysis for fine-grained clay particles. Geotechnical Testing Journal, 2000, 23(4): 487–495
13. GB/T 50145. Standard for Engineering Classification of Soil. Beijing: China Plannig Press, 2007 (in Chinese)
14. ISO 14688-1. Geotechnical Investigation and Testing-Identification and Classification of Soil—Part 1: Identification and Description. London: British Standards Institution, 2018
15. Geospec 3. Model Specification for Soil Testing. Hong Kong (China): Civil Engineering and Development Department, 2017
16. Ma S N, Song Y, Liu J W, Kang X Y, Yue Z Q. Extended wet

sieving method for determining of complete particle size distribution of general soil. Journal of Rock Mechanics and Geotechnical Engineering, 2024, 16(1): 242–257

17. Wen B C, Zhang H, Liu S Y, He Q, Zhang C Y. Theory and Techniques of Vibrating Machinery and Their Applications. Beijing: China Science Press, 2010
18. Stachura H. Economics and Performance of Vibratory Screens. Columbos: The American Ceramic Society, 1994: 424–428
19. AADE. Shale Shakers and Drilling Fluid Systems. Houston: Gulf Publishing Company, 1999
20. Guerreiro F S, Gedraite R, Ataíde C H. Residual moisture content and separation efficiency optimization in pilot-scale vibrating screen. Powder Technology, 2016, 287: 301–307
21. Guilayn F, Jimenez J, Rouez M, Crest M, Patureau D. Digestate mechanical separation: Efficiency profiles based on anaerobic digestion feedstock and equipment choice. Bioresource Technology, 2019, 274: 180–189
22. Girardet N, Webster F H. Oats: Chemistry and Technology. 2nd ed. Saint Paul: American Association of Cereal Chemists, 2011, 301–316
23. Decker E A, Rose D J, Stewart D. Processing of oats and the impact of processing operations on nutrition and health benefits. British Journal of Nutrition, 2014, 112: S58–S64
24. Li Y, Liao X, Li W. Combined sieving and washing of multi-metal-contaminated soils using remediation equipment: A pilot-scale demonstration. Journal of Cleaner Production, 2019, 212: 81–89
25. Song Y, Ma S N, Liu J W, Yue Z Q. Laboratory investigation of CDG soil as source of fine aggregates for Portland cement concrete. Construction & Building Materials, 2023, 367: 130226
26. ISO 3310-1. Test Sieves-Technical Requirements and Testing—Part 1: Test Sieves of Metal Wire Cloth. London: British Standards Institution, 2016
27. ASTM E11-26. Standard Specification for Woven Wire Test Sieve Cloth and Test Sieves. West Conshohocken, PA: ASTM International, 2016
28. Jiang J, Liu S, Wen B. Dynamics analysis, selection and calculation on the parameters of a rotary vibrating screen. Transactions of the Canadian Society for Mechanical Engineering, 2016, 40(4): 563–573
29. Zerin I, Datta E. A review article on applications of filter cloth. International Journal of Clothing Science and Technology, 2018, 5: 1–6
30. Sewell R J, Campbell S D G, Fletcher C J N, Lai K W, Kirk P K. The Pre-quaternary Geology of Hong Kong (China). Hong Kong (China): Civil Engineering and Development Department, 2000
31. Yue Z Q, Lee C F, Law K T, Tham L G. Automatic monitoring of rotary-percussive drilling for ground characterization-illustrated by a case example in Hong Kong (China). International Journal of Rock Mechanics and Mining Sciences, 2004, 41(4): 573–612
32. Shang Y, Li L, He W, Zhang L, Li T, Yang Z. Back analysis of long-term stability of a 92 m span ancient quarrying cavern. Journal of Rock Mechanics and Geotechnical Engineering, 2017, 9(2): 350–363
33. Addison R. Geology of Sha Tin. Hong Kong (China) Geological Survey Memoir. Hong Kong (China): Geotechnical Control Office, 1986
34. ISO 14688-2. Geotechnical Investigation and Testing-Identification of Classification of Soil—Part 2: Principles for A Classification. London: British Standards Institution, 2018
35. Liu K S. Some factors affecting sieving performance and efficiency. Powder Technology, 2009, 193(2): 208–213
36. Schneider C A, Rasband W S, Eliceiri K W. NIH Image to ImageJ: 25 years of image analysis. Nature Methods, 2012, 9(7): 671–675
37. Yadav J S, Tiwari S K. The impact of end-of-life tires on the mechanical properties of fine-grained soil: A review. Environment, Development and Sustainability, 2019, 21(2): 485–568
38. Daoud Y, Robert M. Influence of particle size and clay organization on hydraulic conductivity and moisture retention of clays from saline soils. Applied Clay Science, 1992, 6(4): 293–299
39. Chiappone A, Marello S, Scavia C, Setti M. Clay mineral characterization through the methylene blue test: Comparison with other experimental techniques and applications of the method. Canadian Geotechnical Journal, 2004, 41(6): 1168–1178
40. Bergaya F, Lagaly G. Handbook of Clay Science, 2006